



This is a repository copy of *Synthesis of Mono- and Diiron Dithiolene Complexes as Hydrogenase Models by Dithiolene Transfer Reactions, Including the Crystal Structure of $[Ni(S_2C_2Ph_2)_6]$* .

White Rose Research Online URL for this paper:
<http://eprints.whiterose.ac.uk/142886/>

Version: Accepted Version

Article:

Adams, H., Morris, M.J. orcid.org/0000-0001-8802-9147, Robertson, C.C. orcid.org/0000-0002-1419-9618 et al. (1 more author) (2019) Synthesis of Mono- and Diiron Dithiolene Complexes as Hydrogenase Models by Dithiolene Transfer Reactions, Including the Crystal Structure of $[Ni(S_2C_2Ph_2)_6]$. *Organometallics*, 38 (3). pp. 665-676. ISSN 0276-7333

<https://doi.org/10.1021/acs.organomet.8b00852>

This document is the Accepted Manuscript version of a Published Work that appeared in final form in *Organometallics*, copyright © American Chemical Society after peer review and technical editing by the publisher. To access the final edited and published work see <https://doi.org/10.1021/acs.organomet.8b00852>

Reuse

Items deposited in White Rose Research Online are protected by copyright, with all rights reserved unless indicated otherwise. They may be downloaded and/or printed for private study, or other acts as permitted by national copyright laws. The publisher or other rights holders may allow further reproduction and re-use of the full text version. This is indicated by the licence information on the White Rose Research Online record for the item.

Takedown

If you consider content in White Rose Research Online to be in breach of UK law, please notify us by emailing eprints@whiterose.ac.uk including the URL of the record and the reason for the withdrawal request.



eprints@whiterose.ac.uk
<https://eprints.whiterose.ac.uk/>

**Synthesis of Mono- and Diiron Dithiolene Complexes as Hydrogenase Models by
Dithiolene Transfer Reactions, Including the Crystal Structure of $[\{\text{Ni}(\text{S}_2\text{C}_2\text{Ph}_2)\}_6]$**

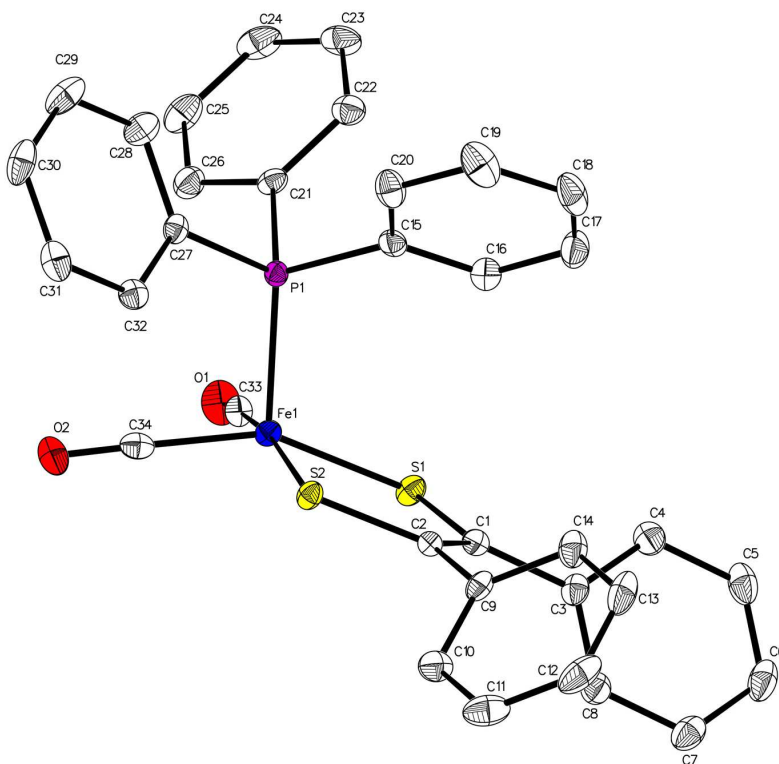
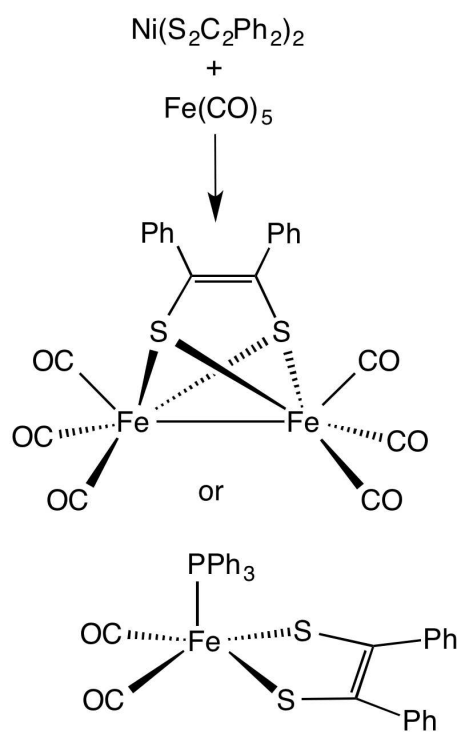
Harry Adams, Michael J. Morris,* Craig C. Robertson and Helen C. I. Tunnicliffe

Department of Chemistry, University of Sheffield,
Sheffield S3 7HF, U.K.

* Corresponding author. E-mail: M.Morris@sheffield.ac.uk

M. J. Morris ORCID: 0000-0001-8802-9147

Table of Contents graphic



Abstract

The dithiolene transfer reaction between the nickel bis(dithiolene) complex $[\text{Ni}(\text{S}_2\text{C}_2\text{Ph}_2)_2]$ and iron carbonyls has been reinvestigated and the conditions for the production of the dinuclear product $[\text{Fe}_2(\mu\text{-S}_2\text{C}_2\text{Ph}_2)(\text{CO})_6]$ have been optimised. Interception of a purple intermediate, thought to be $[\text{Fe}(\text{CO})_3(\text{S}_2\text{C}_2\text{Ph}_2)]$, in the reaction of $[\text{Fe}(\text{CO})_5]$ with $[\text{Ni}(\text{S}_2\text{C}_2\text{Ph}_2)_2]$ by the addition of PPh_3 affords the new dark blue mononuclear complex $[\text{Fe}(\text{CO})_2(\text{PPh}_3)(\text{S}_2\text{C}_2\text{Ph}_2)]$ in good yield. The fate of the nickel dithiolene fragments in these reactions has also been established by crystallographic characterisation of the hexamer $[\{\text{Ni}(\text{S}_2\text{C}_2\text{Ph}_2)\}_6]$ and the trinuclear cluster $[\text{Ni}_3(\mu\text{-S}_2\text{C}_2\text{Ph}_2)_3(\text{PPh}_3)_2]$. The substitution reactions of $[\text{Fe}_2(\mu\text{-S}_2\text{C}_2\text{Ph}_2)(\text{CO})_6]$ with PPh_3 in the presence of Me_3NO to give monosubstituted $[\text{Fe}_2(\mu\text{-S}_2\text{C}_2\text{Ph}_2)(\text{CO})_5(\text{PPh}_3)]$ and disubstituted $[\text{Fe}_2(\mu\text{-S}_2\text{C}_2\text{Ph}_2)(\text{CO})_4(\text{PPh}_3)_2]$ are also reported.

Introduction

It is now generally recognised that the dwindling reserves of fossil fuels and the impact of rising atmospheric CO_2 on the global climate pose a dual threat to the continued advancement of the human race. One of the most promising solutions to these problems is to use the almost inexhaustible energy source, the sun, to power the photochemical splitting of water into hydrogen and oxygen: the former could then be used as a sustainable, green fuel since the only product of its combustion is water. The development of the 'hydrogen economy' faces many technological challenges, not least in its storage, transport and efficiency of utilisation; however the effective production of dihydrogen from water remains a key problem in this endeavour. Attention has mainly focused on the reduction of protons to dihydrogen ($4\text{H}^+ + 4\text{e}^- \rightarrow 2\text{H}_2$) rather than the associated oxidation ($2\text{H}_2\text{O} \rightarrow \text{O}_2 + 4\text{H}^+ + 4\text{e}^-$). Although platinum is a good catalyst for this reaction, its expense and long term unsustainability prompt the search for cheaper alternatives involving more earth-abundant metals.

Nature has solved this problem in typically efficient fashion with the evolution of hydrogenase enzymes that can catalyse the production of H_2 from protons and electrons with extremely high turnovers ($> 9000 \text{ s}^{-1}$) and low overpotentials.¹ Two types of hydrogenase, the $[\text{FeFe}]$ and $[\text{NiFe}]$, that occur in certain bacteria and primitive archaea, are of most interest: the elucidation of the structures of their active sites (shown in Figure 1) has led to efforts by many

synthetic chemists to replicate the unusual structural features and functionality involved, with some success.²⁻⁷

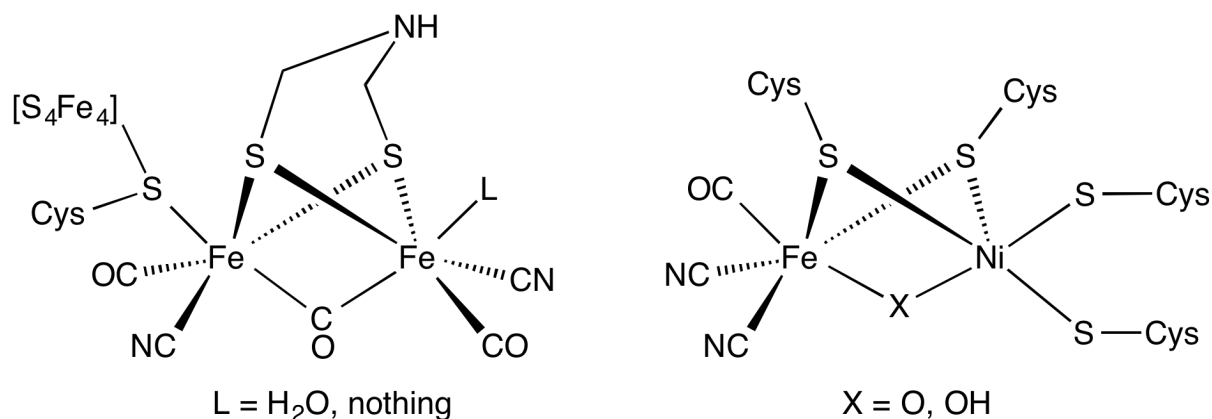


Figure 1. Structures of the dinuclear active sites of [FeFe]- and [NiFe]-hydrogenase enzymes.

Diiron complexes that contain two bridging sulfur-based ligands are very common, if not inevitable, products of the reaction of iron carbonyls with sulfur-containing reagents.⁸ Of the hundreds of hydrogenase active site models prepared, the vast majority involve compounds with this structural motif, particularly $[\text{Fe}_2(\mu\text{-SCH}_2\text{XCH}_2\text{S})(\text{CO})_6]$ ($\text{X} = \text{CH}_2, \text{O}, \text{NH}$), and their various phosphine-substituted derivatives (Figure 2).⁹⁻¹⁴ The ready accessibility of this unit also enables the incorporation of additional moieties of interest, for example redox-active components, light-harvesting antennae or water-solubilizing sidechains.¹⁵⁻²² Although a number of these systems do catalyse the production of H₂ from H⁺, they generally do so only at a large overpotential, in strongly acid solution (e.g. HClO₄ or CF₃CO₂H) and at moderate turnover rates.²³⁻²⁵

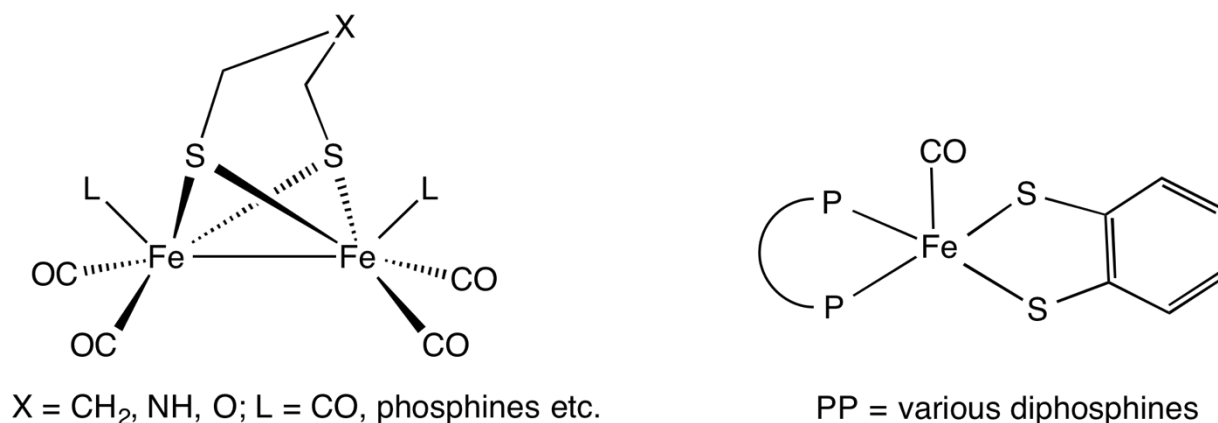


Figure 2. Typical structures of di- and mononuclear models for the active site of the [FeFe]-hydrogenase.

In a more recent development, several groups have explored the use of the more rigid 1,2-benzenedithiolate (bdt) or 3,4-toluenedithiolate (tdt) ligands as the bridging group.²⁶⁻³¹ Moreover, mononuclear iron complexes containing these unsaturated ligands have shown good activity for catalytic proton reduction. This is particularly the case for 5-coordinate complexes of the type $[\text{Fe}(\text{bdt})(\text{CO})(\text{L}_2)]$ where L_2 is a diphosphine ligand (Figure 2).³²⁻³⁹ It should also be mentioned that bdt complexes of other metals, notably cobalt, nickel and molybdenum, have also shown activity for proton reduction.⁴⁰⁻⁴⁵

Over fifty years after the initial breakthroughs of the 1960s, the efficient synthesis of transition metal dithiolene complexes continues to be an important objective in inorganic chemistry.⁴⁶ We were therefore interested in exploring iron complexes similar to those in Figure 2 but containing related dithiolene ligands to take advantage of the unique properties conferred by the non-innocence of these ligands, in particular the accessibility of a range of redox states and the possibility of incorporating additional redox-active substituents.

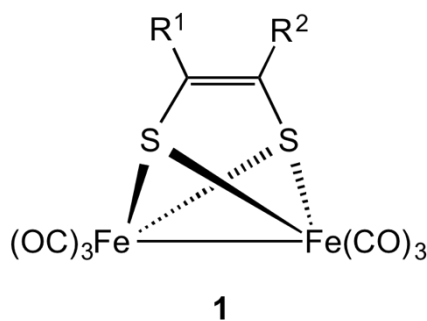


Figure 3. Structure of diiron hexacarbonyl dithiolene complexes.

The bridging dithiolene complexes $[\text{Fe}_2(\mu\text{-SCR}^1=\text{CR}^2\text{S})(\text{CO})_6]$ **1** (Figure 3) form a subset of the class of sulfur-bridged diiron compounds. Several synthetic routes to these exist, such as the reaction of iron carbonyls with bis(trifluoromethyl)dithiete ($\text{R}^1 = \text{R}^2 = \text{CF}_3$),^{47,48} with dithiins ($\text{R}^1 = \text{Ph}$, $\text{R}^2 = \text{H}$ or Ph)⁴⁹ or with dithiooxamides ($\text{R}^1 = \text{R}^2 = \text{NEt}_2$).⁵⁰ Alternatively the complex $[\text{Fe}_2(\mu\text{-S}_2)(\text{CO})_6]$ can be treated with activated alkynes under UV irradiation ($\text{R}^1 = \text{R}^2 = \text{CO}_2\text{Me}$, CF_3)^{51,52} or with the acetylide anions $\text{R}^1\text{C}\equiv\text{C}^-$ followed by protonation of the intermediates ($\text{R}^1 = \text{H}$, Ph , Me ,

Bu, C₅H₁₁, SiMe₃, R² = H).⁵³ Schollhammer and co-workers demonstrated that one of these complexes, with R¹ = R² = CO₂Me, undergoes two reversible electrochemical reductions and is able to reduce protons catalytically.⁵²

The preparation of certain complexes of type **1** (R¹ = R² = H, Ph, Me, *p*-C₆H₄Me, *p*-C₆H₄OMe) was also reported by Schrauzer, who employed the reaction between [Fe(CO)₅] and the metal bis(dithiolenes) [M(SCR¹=CR²S)₂] (M = Fe, Co, Ni).⁵⁴ However experimental details were rather minimal, and no yields were given. We have been studying the use of dithiolene transfer reactions in the synthesis of both known and new dithiolene complexes for some years⁵⁵⁻⁵⁷ and were interested in reinvestigating this route to compounds of type **1** as the availability of a large and diverse range of nickel dithiolene complexes might allow the preparation of compounds of this type that are unavailable by any of the previous routes. In this paper we report (i) the optimisation of the dithiolene transfer reaction (ii) the modification of the synthesis to afford mononuclear phosphine-substituted complexes in one step; and (iii) the crystallographic characterisation of the nickel cluster co-products of both reactions.

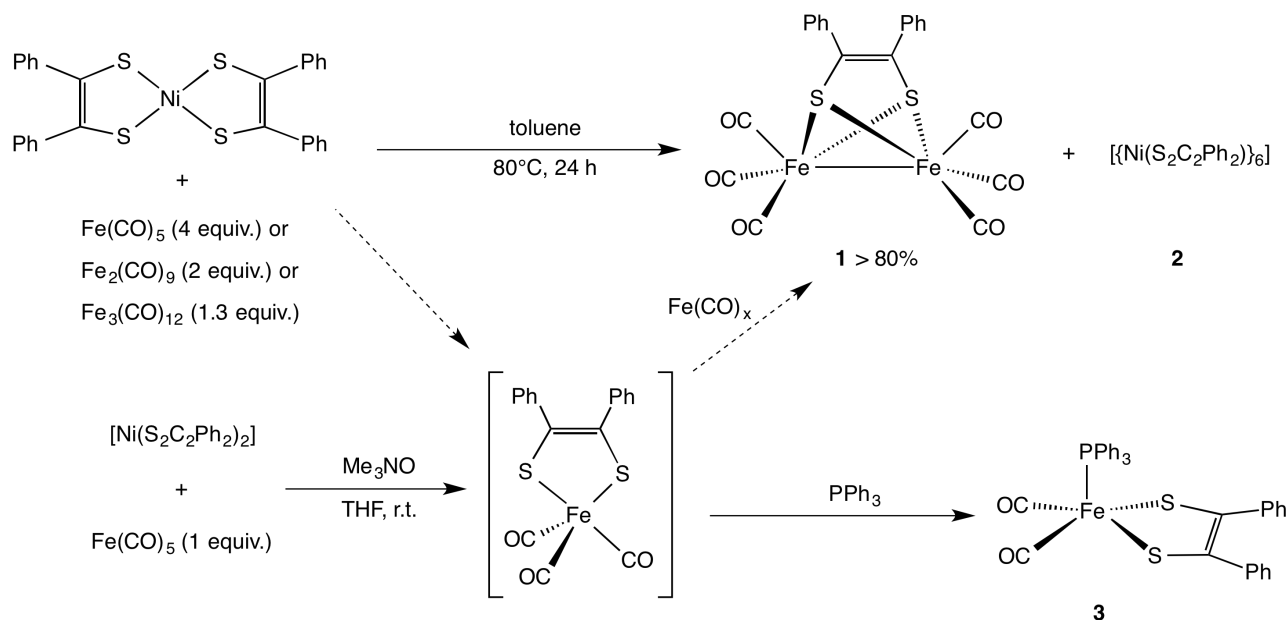
Results and Discussion

Dithiolene transfer reactions: iron complexes

We have concentrated on the complex [Fe₂(μ-S₂C₂Ph₂)(CO)₆] (**1**), firstly because the appropriate precursor nickel bis(dithiolene) complex [Ni(S₂C₂Ph₂)₂] is readily available, and secondly because its spectroscopic data were recently reported by Mousser *et al.* who unexpectedly isolated it in moderate yield from the reaction of [Fe₂(CO)₉] with phenyl dithiobenzoate.⁵⁸ Their paper also includes the X-ray structure determination of the complex, supplementing an earlier one by Weber and Bryan.⁵⁹

In Schrauzer's original method, the bis(dithiolene) complexes [M(S₂C₂Ph₂)₂] (M = Fe, Co, Ni) were heated with a large (~20-fold) excess of [Fe(CO)₅] in refluxing benzene.⁵⁴ We found that heating [Ni(S₂C₂Ph₂)₂] with a four-fold excess of [Fe(CO)₅] in toluene at 80°C overnight produced good yields of **1** (> 80% based on the Ni reagent transferring one dithiolene ligand to the iron center), which can be isolated by chromatography as an air-stable bright orange-red solid and characterised by its IR, mass, ¹H and ¹³C NMR spectra, which match those in the literature (Scheme 1).⁵⁸ The reaction between [Ni(S₂C₂Ph₂)₂] and [Fe(CO)₅] can also be carried out at 75°C in THF in

the presence of Me_3NO (2 equiv.), giving an 88% yield of **1**. It is well known that both $[\text{Fe}_2(\text{CO})_9]$ and $[\text{Fe}_3(\text{CO})_{12}]$ can also serve as sources of iron carbonyl fragments in reactions with sulfur-containing substrates, and as expected the reactions of $[\text{Ni}(\text{S}_2\text{C}_2\text{Ph}_2)_2]$ with either of these reagents under similar conditions also gave good yields of **1** (72% and 98% respectively). In all of these reactions the only other significant product is the hexameric nickel complex **2**, described later.



Scheme 1. Synthesis of the iron dithiolene complexes by dithiolene transfer.

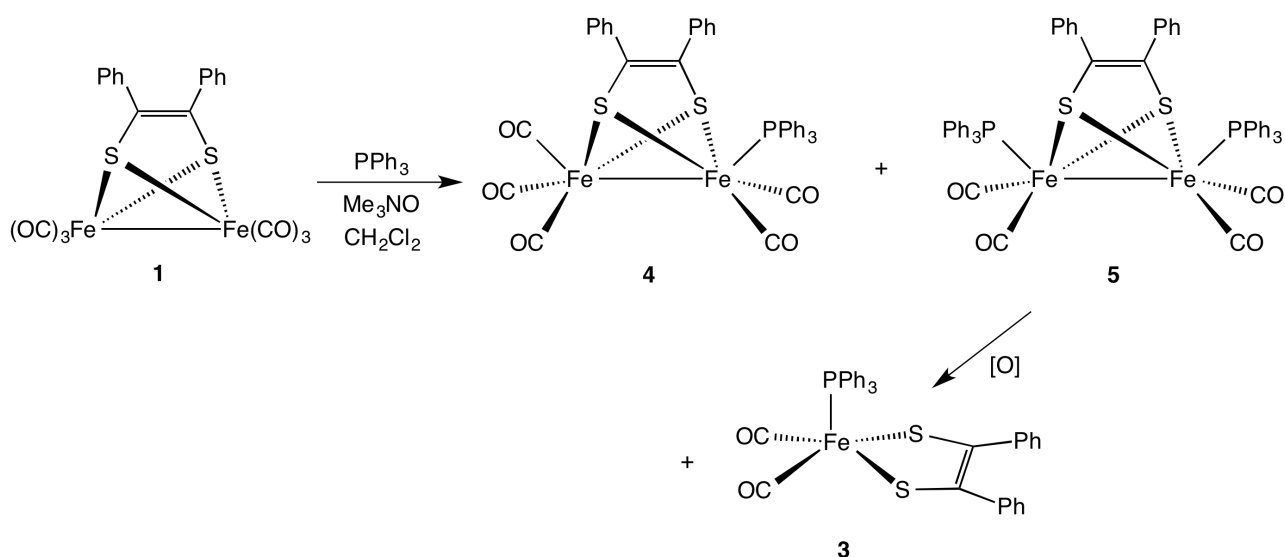
In most of these reactions (except, curiously, the one involving $[\text{Fe}_3(\text{CO})_{12}]$), the reaction mixture initially changed color from green to deep purple, then gradually to orange-brown. The purple complex could not be characterised; although small amounts remained at the end of the reaction and could be collected from the chromatography column, it decomposed to a green residue when the solvent was removed. In the reaction carried out with Me_3NO , the solution rapidly turned dark purple on addition of the amine oxide, evolving gas as it did so. We consider it most likely that the purple intermediate is $[\text{Fe}(\text{CO})_3(\text{S}_2\text{C}_2\text{Ph}_2)]$. Previously Balch and McCleverty have prepared the analogous $[\text{Fe}(\text{CO})_3\{\text{S}_2\text{C}_2(\text{CF}_3)_2\}]$, described as magenta;^{48, 60} although it exhibited a dimeric structure in the solid state,⁶¹ it was shown to react with additional $[\text{Fe}(\text{CO})_5]$ to give $[\text{Fe}_2(\text{CO})_6\{\mu\text{-S}_2\text{C}_2(\text{CF}_3)_2\}]$. The only other isolable species of this type appear to be the dithioamide complexes $[\text{Fe}(\text{CO})_3\{\text{S}_2\text{C}_2(\text{NEt}_2)_2\}]$ and $[\text{Fe}(\text{CO})_3\{\text{S}_2\text{C}_2(\text{NMeCH}_2\text{CH}_2\text{NMe})\}]$, which undergo a similar

reaction.⁵⁰ It therefore appears to be a reasonable proposal that $[\text{Fe}(\text{CO})_3(\text{S}_2\text{C}_2\text{Ph}_2)]$ is an intermediate in the formation of **1** in our reaction.

Both Balch and McCleverty also noted that $[\text{Fe}(\text{CO})_3\{\text{S}_2\text{C}_2(\text{CF}_3)_2\}]$ reacted readily with phosphine ligands to give $[\text{Fe}(\text{CO})_2(\text{L})\{\text{S}_2\text{C}_2(\text{CF}_3)_2\}]$. We therefore wondered if it would be possible to intercept the intermediate by addition of a phosphine ligand before it reacted to give **1**. Addition of triphenylphosphine to the dark purple solution produced from $[\text{Ni}(\text{S}_2\text{C}_2\text{Ph}_2)_2]$ and one equivalent of $[\text{Fe}(\text{CO})_5]$ in the presence of Me_3NO caused an immediate color change to green, and the dark blue substituted complex $[\text{Fe}(\text{CO})_2(\text{PPh}_3)(\text{S}_2\text{C}_2\text{Ph}_2)]$ **3** (*vide infra*) was isolated in 59% yield (Scheme 1). Hence the purple intermediate certainly reacts as if it were $[\text{Fe}(\text{CO})_3(\text{S}_2\text{C}_2\text{Ph}_2)]$, and we are currently exploring this procedure as a useful route to other mononuclear iron carbonyl dithiolene derivatives.

Substitution reactions of 1 ($R^1 = R^2 = \text{Ph}$) with PPh_3 .

No reaction occurred on stirring a dichloromethane solution of **1** ($R^1 = R^2 = \text{Ph}$) with one or two equivalents of PPh_3 at room temperature. However on addition of one or two equivalents of Me_3NO , the solution darkened rapidly and three products could be isolated by column chromatography or TLC: the red monosubstituted complex $[\text{Fe}_2(\mu\text{-S}_2\text{C}_2\text{Ph}_2)(\text{CO})_5(\text{PPh}_3)]$ **4**, the brown disubstituted complex $[\text{Fe}_2(\mu\text{-S}_2\text{C}_2\text{Ph}_2)(\text{CO})_4(\text{PPh}_3)_2]$ **5** and the blue mononuclear species $[\text{Fe}(\text{CO})_2(\text{PPh}_3)(\text{S}_2\text{C}_2\text{Ph}_2)]$ **3** (Scheme 2). Compound **5** is air-sensitive and decomposes to **3** during purification, but this does not account for the total amount of this product: it is already present in the reaction mixture before work-up. Compounds **3-5** were readily characterised by their spectroscopic data and by comparison to other related species. For example, Dixneuf and co-workers have previously shown that the analogous disubstituted tetrathiooxalate complexes $[\text{Fe}_2\{\mu\text{-S}_2\text{C}_2(\text{SR})_2\}(\text{CO})_4(\text{PPh}_3)_2]$ ($R = \text{Me}, \text{Et}$), prepared by reduction of $[\text{Fe}(\text{CO})_2(\text{PPh}_3)_2(\text{CS}_2\text{R})]^+$, also decompose to $[\text{Fe}\{\text{S}_2\text{C}_2(\text{SR})_2\}(\text{CO})_2(\text{PPh}_3)]$ on exposure to air; they also crystallographically characterised both the dinuclear and mononuclear products for $R = \text{Me}$.⁶² Numerous mono- and di-substituted derivatives of the toluene-dithiolate complex $[\text{Fe}_2(\mu\text{-S}_2\text{C}_6\text{H}_3\text{Me})(\text{CO})_6]$ and the 1,3-propanedithiolate complex $[\text{Fe}_2(\mu\text{-S}_2\text{C}_3\text{H}_6)(\text{CO})_6]$ with PPh_3 have been prepared and structurally characterised.^{10, 26, 27} By analogy with these compounds, we expect the phosphine ligands to occupy the apical positions in **4** and **5**, as shown in Scheme 2.^{62, 63}



Scheme 2. Substitution reaction of complex **1** with PPh_3 .

The crystal structure of mononuclear complex **3** was determined and is shown in Figure 4, with bond lengths and angles summarised in the caption. The complex is best described as adopting a square-based pyramidal geometry with the phosphine ligand in the apical position; the trigonality index, τ , = 0.24.⁶⁴ Interestingly this is subtly different to the structure of $[\text{Fe}\{\text{S}_2\text{C}_2(\text{SMe})_2\}(\text{CO})_2(\text{PPh}_3)]$, which, although still square based pyramidal with $\tau = 0.29$, had a CO ligand as the apical group.⁶² The origin of this difference may be steric, as it places the bulky phosphine ligand further away from the diphenyldithiolene. It has been known for many years that a similar ruthenium complex, $[\text{Ru}(\text{CO})(\text{PPh}_3)_2\{\text{S}_2\text{C}_2(\text{CF}_3)_2\}]$ exists as two interconverting square pyramidal isomers: one violet with an apical phosphine ligand and the other orange with the CO ligand in the apical position; very recently the two forms have been shown to interconvert *via* an observable trigonal bipyramidal intermediate.^{48, 65-68}

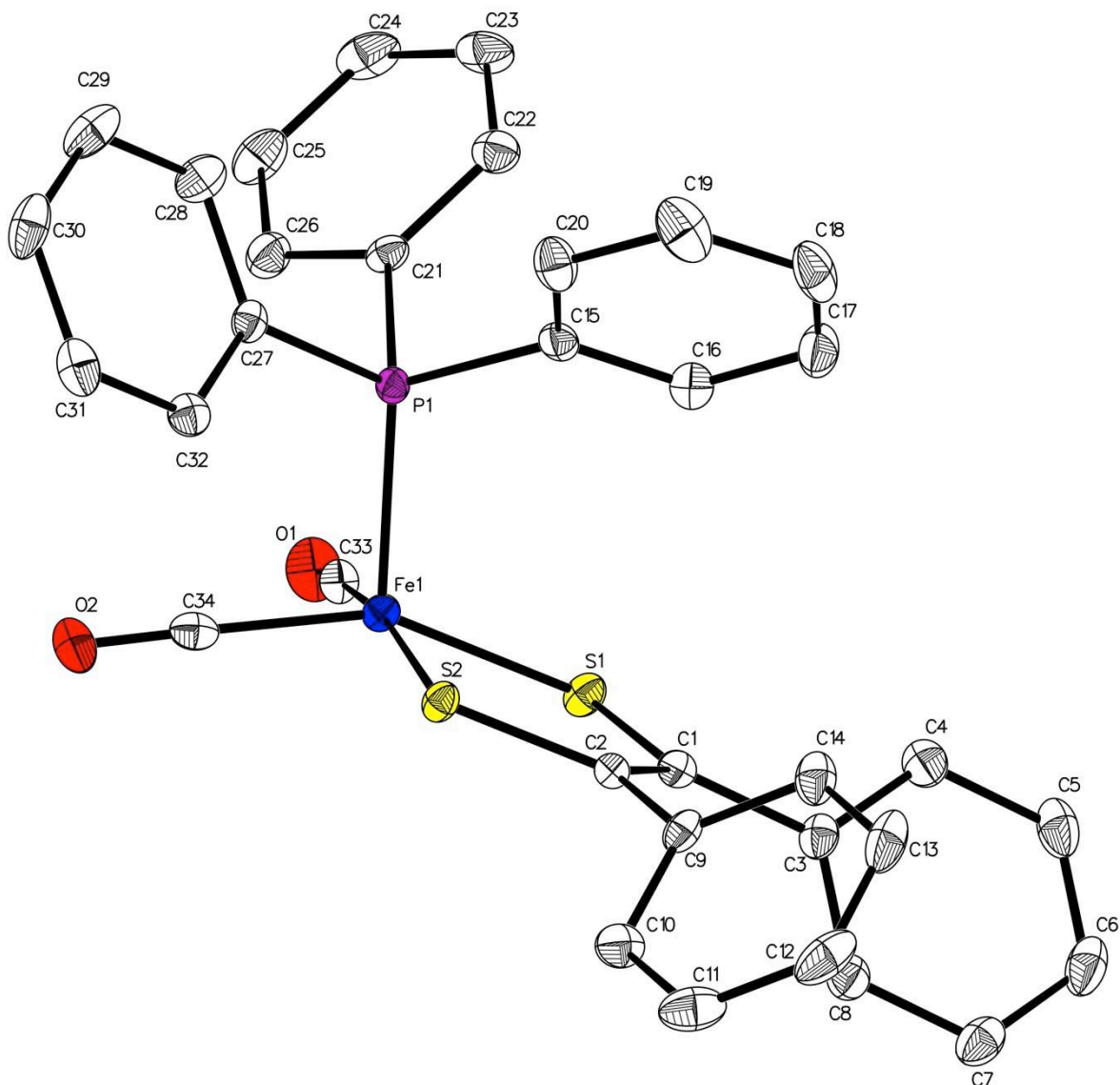


Figure 4. Molecular structure of $[\text{Fe}(\text{CO})_2(\text{PPh}_3)(\text{S}_2\text{C}_2\text{Ph}_2)]$ **3** in the crystal. Selected bond lengths (Å) and angles (°): Fe(1)–S(1) 2.1761(5), Fe(1)–S(2) 2.1942(5), Fe(1)–P(1) 2.2158(6), Fe(1)–C(33) 1.791(2), Fe(1)–C(34) 1.791(2), C(33)–O(1) 1.142(2), C(34)–O(2) 1.142(2), C(1)–C(2) 1.371(3); S(1)–Fe(1)–S(2) 88.18(2), S(1)–Fe(1)–P(1) 113.52(2), S(2)–Fe(1)–P(1) 94.05(2), C(33)–Fe(1)–S(1) 84.57(6), C(33)–Fe(1)–S(2) 167.01(6), C(33)–Fe(1)–P(1) 98.72(6), C(33)–Fe(1)–C(34) 91.27(9), C(34)–Fe(1)–S(1) 152.59(6), C(34)–Fe(1)–S(2) 90.23(6), C(34)–Fe(1)–P(1) 93.89(6).

In a very recent paper a contrasting result to ours has been obtained by Mousser and co-workers.⁶⁹ Treatment of **1** with P(OMe)₃ in toluene at 45°C gave mono- and di-substituted dinuclear species analogous to **4** and **5**, but instead of a monosubstituted analog of **3**, the disubstituted mononuclear complex [Fe(CO){P(OMe)₃}₂(S₂C₂Ph₂)] was obtained. This compound adopts a structure somewhat more towards trigonal bipyramidal ($\tau = 0.44$) in which both phosphite ligands occupy equatorial positions, the dithiolene ligand spans the axial and equatorial sites, and the CO is in the remaining axial position. Clearly the ligand arrangement in these mononuclear species is very dependent on the steric and electronic properties of the ligands concerned. Our attempts to induce a second substitution in [Fe(CO)₂(PPh₃)(S₂C₂Ph₂)] were hampered by the fact that heating the complex in refluxing toluene, either alone or with PPh₃, unexpectedly caused its almost quantitative transformation into the known bis(dithiolene) complex [Fe(PPh₃)(S₂C₂Ph₂)₂].^{54, 70} In contrast, [Fe(CO)₃{S₂C₂(CF₃)₂}] is known to undergo a second phosphine substitution reaction under thermal conditions to give [Fe(CO)(L)₂{S₂C₂(CF₃)₂}]^{48, 60}

Since it appeared that **1** may be formed by the reaction of [Fe(CO)₃(S₂C₂Ph₂)] with additional [Fe(CO)₅], we also attempted to prepare the monosubstituted complex **4** by the reaction of complex **3** with an excess of [Fe(CO)₅] and Me₃NO. Although **4** was formed in 39% yield, the major product was the unsubstituted complex **1** (51%). No trace of the purple band that we propose to be [Fe(CO)₃(S₂C₂Ph₂)] was observed in this reaction; it therefore seems likely that the initial product is indeed **4**, but the PPh₃ ligand is then replaced by CO to give **1**.

The electrochemical behavior of **1** was reported recently.⁶⁹ The cyclic voltammogram of complex **3** is shown in Figure 5. The compound displays a reversible reduction wave at - 1.359 V (vs. Fc/Fc⁺) as well as some more complex oxidation behavior. Addition of successive 100-equivalent aliquots of acetic acid did cause a small but consistent increase in the current of the reduction wave (see Supplementary Information) but we conclude that the ability of **3** to catalyse the proton reduction reaction under these conditions is weak at best.

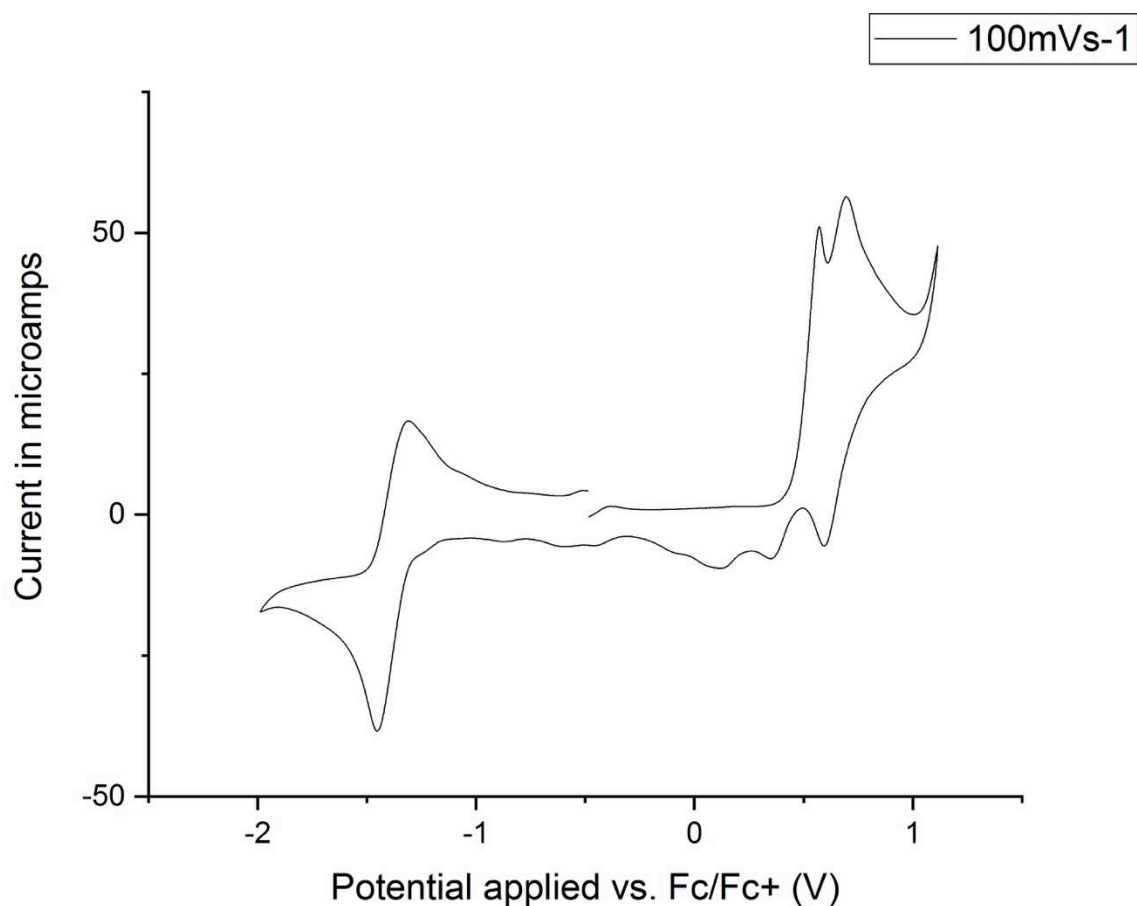


Figure 5. Cyclic voltammogram of complex **3** in CH₂Cl₂ solution (room temperature, scan rate 100 mVs⁻¹).

Dithiolene transfer reactions: nickel complexes

In addition to the iron complexes produced in the dithiolene transfer reactions, we have also characterised the nickel clusters that occur as co-products. In all of the dithiolene transfer reactions giving **1**, the brown complex [$\{\text{Ni}(\text{S}_2\text{C}_2\text{Ph}_2)\}_6$] **2** was eluted as a co-product in a yield similar to that of **1** (when calculated on the basis of the starting nickel complex). It therefore appears that only one dithiolene ligand from the nickel starting material is transferred to the iron center, and the remaining Ni(S₂C₂Ph₂) fragments assemble into the hexamer. This compound, formulated at the time as [$\{\text{Ni}(\text{S}_2\text{C}_2\text{Ph}_2)\}_n$], was first isolated in the 1960s by Schrauzer in the reactions of [Ni(S₂C₂Ph₂)₂] with alkynes. It was suggested that only one dithiolene ligand per complex reacted (to give thiophenes), leaving the remaining Ni(S₂C₂Ph₂) fragment to associate into a brown complex that they initially described as a tetramer ($n = 4$).⁷¹⁻⁷³ In the following year they isolated the

same compound as a by-product in dithiolene transfer reactions between $[\text{Ni}(\text{S}_2\text{C}_2\text{Ph}_2)_2]$ and $[\text{M}(\text{CO})_6]$ ($\text{M} = \text{Cr}, \text{Mo}, \text{W}$);⁷⁴ much later Holm and co-workers also observed it in the related reaction of $[\text{Ni}(\text{S}_2\text{C}_2\text{Ph}_2)_2]$ with $[\text{M}(\text{CO})_3(\text{NCMe})_3]$ ($\text{M} = \text{Mo}, \text{W}$) and described it as probably polymeric.^{75,76} The reaction of $[\text{Ni}(\text{S}_2\text{C}_2\text{Ph}_2)_2]$ with nickelocene to give $[\text{CpNi}(\text{S}_2\text{C}_2\text{Ph}_2)]$ also produced complex **2**, and in this case an ion was observed in the mass spectrum at m/z 1806, indicating a hexameric structure.⁷⁷ We have previously observed its formation in reactions of $[\text{Ni}(\text{S}_2\text{C}_2\text{Ph}_2)_2]$ with carbonyl-containing substrates,⁵⁵ though interestingly in other cases involving dithiolene transfer to complexes containing halides (such as $[\text{CpMo}(\text{CO})_3\text{Cl}]$ or $[\text{RuCl}_2(\text{PPh}_3)_3]$) it was not produced, and the fate of the nickel in these reactions remains unclear.^{56,57}

Bis- or tris-dithiolene complexes of the general formula $[\text{M}(\text{S}_2\text{C}_2\text{R}_2)_2]$ or $[\text{M}(\text{S}_2\text{C}_2\text{R}_2)_3]$ are relatively common and can be prepared for most of the transition metals.⁴⁶ However monodithiolene complexes of the general type $[\text{M}(\text{S}_2\text{C}_2\text{R}_2)]_n$ with a 1:1 metal:dithiolene ratio are much rarer, and are confined to four structurally characterised compounds: the dimeric $[\{\text{Tl}(\text{bdt})\}_2]^{2-}$ ($\text{bdt} = 1,2\text{-benzenedithiolate}, \text{S}_2\text{C}_6\text{H}_4$),⁷⁸ the tetramer $[\{\text{Ag}(\text{mnt})\}_4]^{4-}$, [$\text{mnt} = 1,2\text{-maleonitriledithiolate}, \text{S}_2\text{C}_2(\text{CN})_2$]⁷⁹ and two hexameric palladium complexes discussed in more detail below. It was therefore of interest to structurally characterise **2**, which is the most readily available member of this series.

Crystallisation of **2** was effected by diffusion of light petroleum into a dichloromethane solution at room temperature, giving brown needles. The structure is depicted in Figure 6 and is based on an octahedral arrangement of six nickel atoms, each of which is in a square planar coordination environment; if an imaginary cube is constructed such that the nickel atoms lie in the centers of its faces, the sulfur atoms of the dithiolene ligands occupy the centers of each edge of this cube. Unique nickel atom Ni(1) at the top of the diagram, bears two chelating dithiolene ligands, the sulfur atoms of which each bridge to one of the four nickel atoms in the equatorial positions [Ni(3)-Ni(6)]. The other unique nickel atom, Ni(2), at the bottom of the octahedron, is bonded to four different dithiolene ligands, each of which bridges to one of the equatorial nickels, which are themselves therefore ligated by three different dithiolenes. All of the Ni–Ni distances are greater than 3.0 Å, precluding any significant metal-metal bonding. The Ni–S distances within a chelating dithiolene ring lie in the range 2.16–2.19 Å, whereas the bridging Ni–S distances are longer, between 2.23 and 2.27 Å.

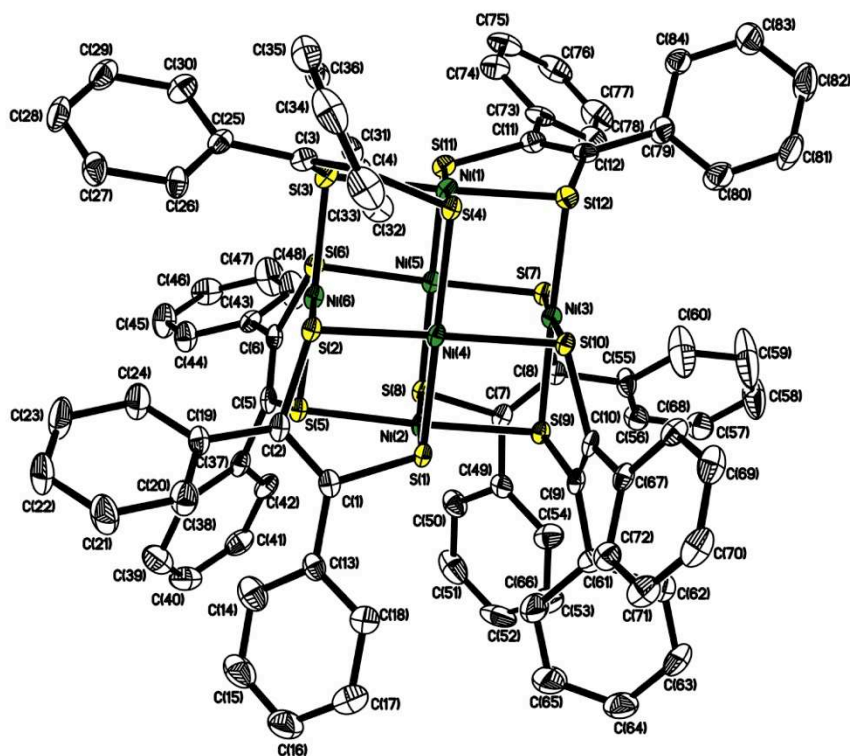


Figure 6. Molecular structure of complex **2** in the crystal.

Two closely related hexanuclear palladium dithiolene complexes have been described. The first of these, $[\text{Pd}\{\text{S}_2\text{C}_2(\text{CO}_2\text{Me})_2\}]_6$, was isolated by Stiefel from the reaction of $[\text{PdCl}_2(\text{NCMe})_2]$ with $[\text{Zn}(\text{tmeda})\{\text{S}_2\text{C}_2(\text{CO}_2\text{Me})_2\}]$.⁸⁰ Its structure consists of an octahedral Pd_6 core bridged by dithiolene ligands but in a subtly different way such that the structure has S_6 symmetry and each Pd is bonded to three different dithiolene ligands. More recently, Rawson and co-workers have explored the oxidative addition of tetrathiocins to Pd(0) complexes, producing the benzenedithiolate cluster $[\text{Pd}\{\text{S}_2\text{C}_6\text{H}_2(\text{OMe})_2\}]_6$, which has the same arrangement of the dithiolate ligands as in **2**.⁸¹

In the solid state structure of **2** there is a 2-fold axis of symmetry which renders pairs of dithiolene ligands equivalent; within each dithiolene ligand the two carbons are not equivalent. In the ^{13}C NMR spectrum one would therefore expect to see six signals of equal intensity for the dithiolene carbons, and the same for the *ipso* carbons of the phenyl substituents. A total of twelve

signals are observed in this region, implying that the solid state structure is maintained in solution. The molecule is chiral: as shown in Figure 7, when viewed from above Ni(1) the dithiolene ligands of each sulfur in the equatorial plane bridge to the nickel atom in a leftward direction, whereas its enantiomer would have the opposite direction (the molecule of Rawson's Pd₆ complex depicted in that paper is the right-handed enantiomer).⁸¹

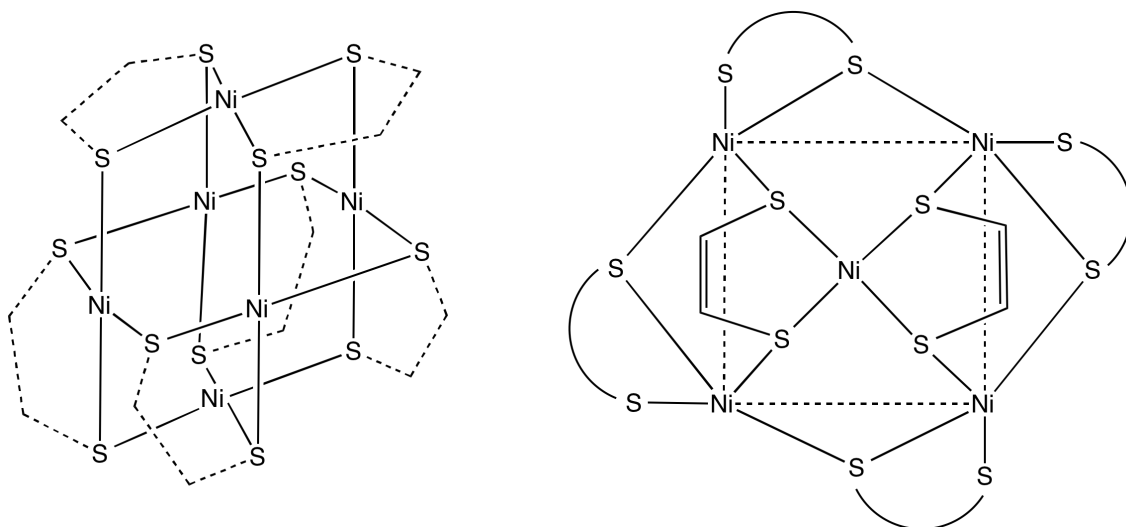


Figure 7. Schematic view of the framework of cluster **2** from the side (left) and top (right) of the molecule.

The cyclic voltammogram of hexamer **2** is shown in Figure 8. The complex displays two reversible reduction waves at -1.028V and -1.593V (vs. Fc/Fc^+) as well as two smaller oxidation waves at 0.277V and 0.470V , followed by a larger wave (which may consist of two closely spaced oxidations) at 0.962V . It is interesting to note that Stiefel's $[\text{Pd}\{\text{S}_2\text{C}_2(\text{CO}_2\text{Me})_2\}]_6$ cluster showed four reversible reduction waves whereas Rawson's Pd₆ cluster showed only two reductions and two oxidations (the oxidation behavior of Stiefel's cluster was not reported).^{80,81}

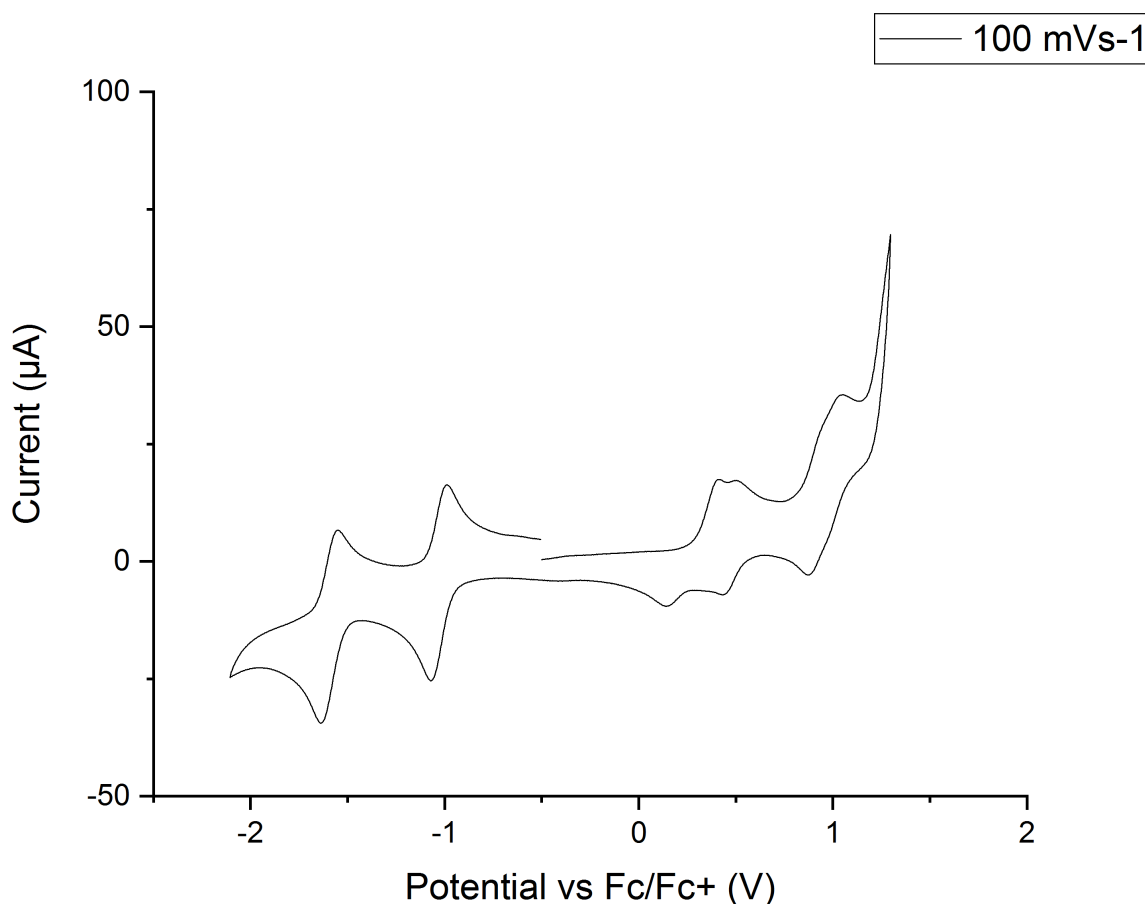


Figure 8. Cyclic voltammogram of complex **2** in CH₂Cl₂ solution (room temperature, scan rate 100 mVs⁻¹).

The reactions carried out in the presence of PPh₃ to give **3** did not however produce the hexamer **2**. Instead a new cluster, [Ni₃(μ-S₂C₂Ph₂)₃(PPh₃)₂] **6** (Figure 9) was isolated in low yield as a green solid; its mass spectrum showed a molecular ion centered on *m/z* 1426. The single crystal X-ray structure of this complex is shown in Figure 10, with important bond lengths and angles detailed in the caption. The structure consists of an equilateral triangle of nickel atoms; Ni(1) and Ni(2), each of which bears a phosphine ligand, are symmetrically bridged by sulfur atoms S(5) and S(6) of the unique dithiolene ligand. In contrast Ni(3) is ligated by two chelating dithiolenes, which are bridging in the unusual μ₃ coordination mode: one sulfur of each ligand bridges to Ni(1) and the other to Ni(2). The bridging of these two dithiolenes is much more asymmetric: the average Ni(3)-S distance is 2.162 Å, whereas the average Ni(1)/Ni(2) bond distance to the same four sulfurs is 2.2905 Å. The geometry about Ni(3) is thus distorted square planar whereas the other two metals

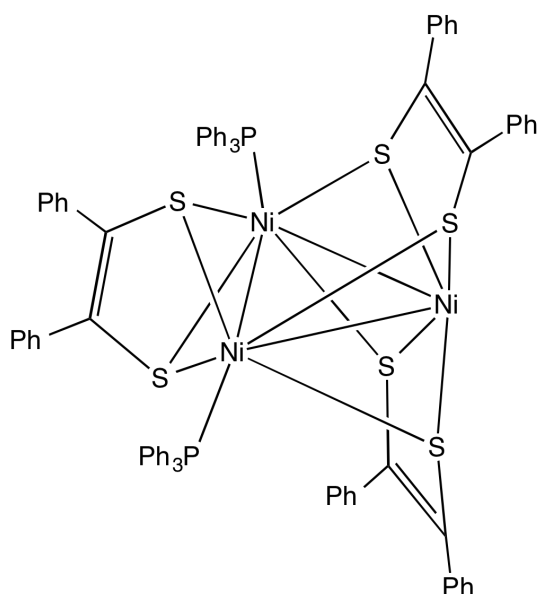


Figure 9. Structure of $[\text{Ni}_3(\mu\text{-S}_2\text{C}_2\text{Ph}_2)_3(\text{PPh}_3)_2]$ **6**.

have a square pyramidal coordination environment. Although the cluster has 52 electrons as opposed to the more usual 48 (which corresponds to an 18-electron configuration for each metal with three M–M single bonds), the three Ni–Ni distances are all similar [2.4914(7)–2.5305(9) Å] and well within the range observed for a bonding interaction, and the Ni–Ni–Ni angles are close to 60°. The μ_3 -coordination of the dithiolene ligand, in which the ligand largely retains its planarity, has been observed previously in mixed-metal clusters by Nishihara.^{82,83} Moreover two structurally very similar benzenedithiolate clusters, $[\text{Ni}_3(\mu\text{-bdt})_3(\text{PPh}_3)_2]$ and $[\text{Ni}_3(\mu\text{-bdt})_3(\text{PPh}_2\text{Me})_2]$, both of which also feature relatively short Ni–Ni distances, have been reported in the literature.^{84,85}

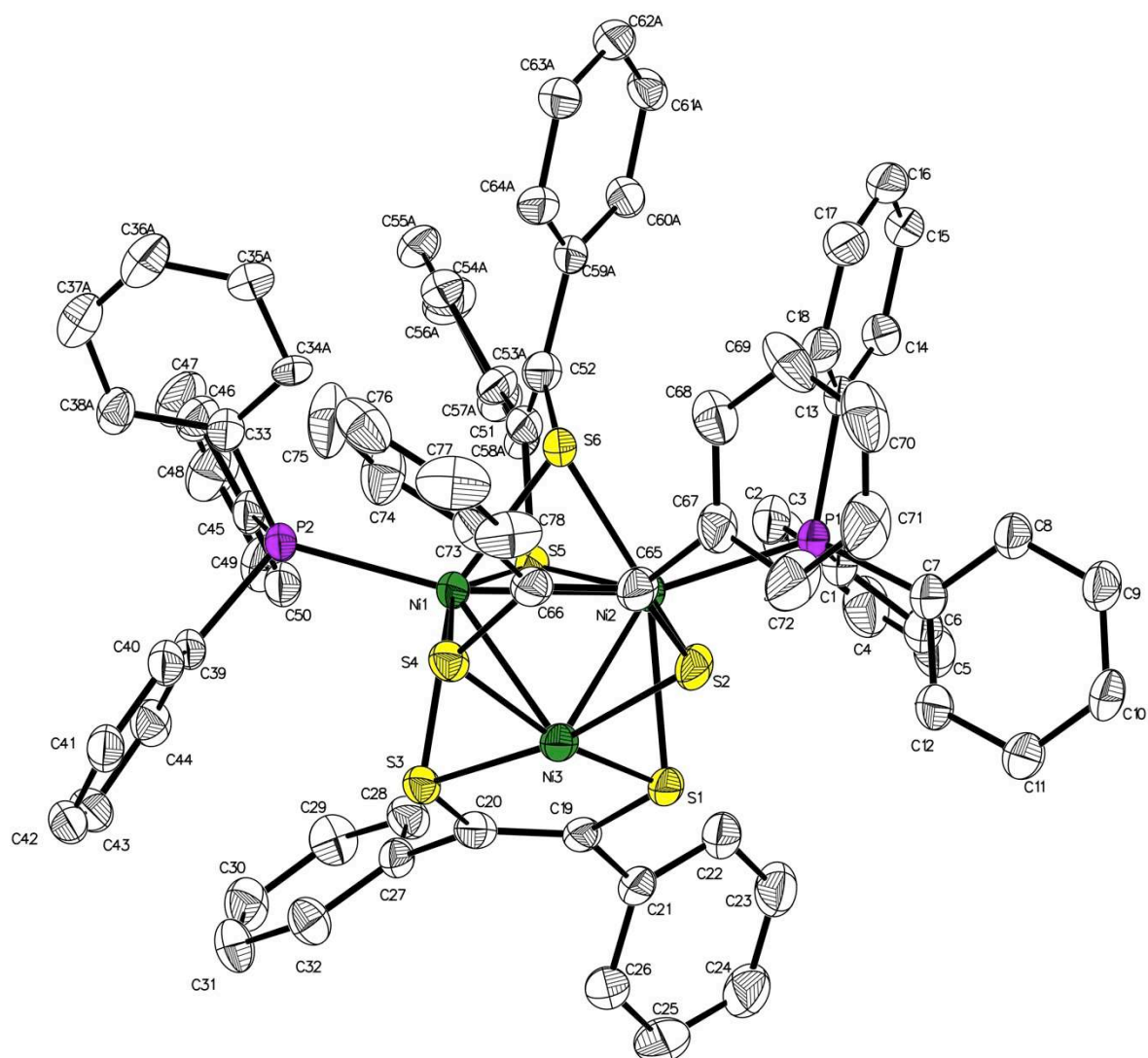


Figure 10. Molecular structure of complex **6** in the crystal. Selected bond lengths (Å): Ni(1)–Ni(2) 2.4914(7), Ni(1)–Ni(3) 2.5125(8), Ni(2)–Ni(3) 2.5305(9), Ni(2)–S(1) 2.4767(12), Ni(3)–S(1) 2.1566(13), Ni(2)–S(2) 2.4500(14), Ni(3)–S(2) 2.1629(12), Ni(1)–S(3) 2.4959(12), Ni(3)–S(3) 2.1621(11), Ni(1)–S(4) 2.4147(13), Ni(3)–S(4) 2.1657(13), Ni(1)–S(5) 2.2840(13), Ni(2)–S(5) 2.2883(12), Ni(1)–S(6) 2.2975(13) Ni(2)–S(6) 2.2924(12), Ni(1)–P(2) 2.2720(11), Ni(2)–P(1) 2.2759(12), C(19)–C(20) 1.356(6), C(65)–C(66) 1.344(6), C(51)–C(52) 1.374(8).

Cluster **6** is evidently formed by the interception of the Ni(S₂C₂Ph₂) units produced in the dithiolenone transfer reaction by PPh₃, thus preventing them associating further into hexamer **2**. This suggests that a general route to such compounds might involve generating such units in the presence of other phosphines, a possibility we are currently exploring.

Conclusions

We have confirmed that the dithiolene transfer reaction of $[\text{Ni}(\text{S}_2\text{C}_2\text{Ph}_2)_2]$ with iron carbonyls forms a viable route to the dinuclear complex $[\text{Fe}_2(\mu\text{-S}_2\text{C}_2\text{Ph}_2)(\text{CO})_6]$, as described by Schrauzer. Furthermore we have demonstrated that the reaction passes through an intermediate species, thought to be $[\text{Fe}(\text{CO})_3(\text{S}_2\text{C}_2\text{Ph}_2)]$, that can be intercepted by reaction with PPh_3 to give useful yields of $[\text{Fe}(\text{CO})_2(\text{PPh}_3)(\text{S}_2\text{C}_2\text{Ph}_2)]$ in a convenient one-pot synthesis. We are currently exploring the scope of this reaction with other dithiolene ligands and phosphines, and studying the electrochemical and catalytic properties of the resulting five-coordinate complexes.

In addition we have also structurally characterised the hexameric nickel co-product $[\{\text{Ni}(\text{S}_2\text{C}_2\text{Ph}_2)\}_6]$ **2**, a compound commonly observed in dithiolene transfer reactions. More unexpectedly, we have shown that in the presence of PPh_3 , the aggregation of the Ni(dithiolene) fragments can be arrested before they form **2**, giving instead a new trinuclear cluster **6**; in this way it may be possible to synthesize a range of different clusters of intermediate nuclearity by the addition of different ligands.

Experimental

All reactions were performed under an inert atmosphere of argon or nitrogen using Schlenk techniques. Solvents for reactions were purified with a Grubbs-type purification system manufactured by Innovative Technology, Newburyport, MA. Chromatographic separations were carried out on Geduran 60 silica under a positive pressure of nitrogen; columns were initially made up in light petroleum (40-60 °C fraction); polarity was increased by addition of increasing proportions of dichloromethane. The ^1H (400 MHz), ^{13}C NMR (100 MHz) and ^{31}P NMR (162 MHz) spectra were obtained in CDCl_3 solution on a Bruker Avance AVIIIHD machine having an automated sample-changer. Chemical shifts are given on the δ scale relative to SiMe_4 for ^1H and ^{13}C , and relative to 85% H_3PO_4 for ^{31}P . The $^{13}\text{C}\{^1\text{H}\}$ NMR spectra were routinely recorded using an attached proton test technique (JMOD or DEPT-Q pulse sequence). Mass spectra were recorded on Waters LCT instruments operating in electrospray (ES^+) or atmospheric pressure chemical ionisation (AP^+) mode. Solid state IR spectra were recorded neat with a diamond ATR device over the range 4000-400 cm^{-1} , and solution spectra in CH_2Cl_2 solution over the range 2200-1550 cm^{-1} ,

on a Perkin Elmer Spectrum Two instrument. Elemental analyses were carried out by the Microanalytical Service of the Department of Chemistry.

Standard cyclic voltammetry was carried out using an Autolab Potentiostat 100 attached to a computer using NOVA 1.10.5 software to record the data. The data were processed using OriginPro 2018. The experiments were performed at room temperature in a glass sample tube using a glassy carbon working electrode, a platinum wire counter electrode and a Ag/AgCl reference electrode under a nitrogen atmosphere. The solvent was dichloromethane containing $[\text{NBu}_4][\text{PF}_6]$ (0.4 M) as supporting electrolyte. The compound concentration was 2 mM unless stated otherwise. The solution was saturated with N_2 by bubbling the gas into the solution for a minimum of 10 minutes. All redox potentials quoted in the figures and results and discussion sections are vs. the ferrocene-ferrocenium couple (Fc/Fc^+). Scan rates of 20–500 mVs^{-1} were used, with the figure caption stating which was used to obtain the traces shown.

All chemicals were purchased from Sigma-Aldrich UK with the exception of $[\text{Fe}_2(\text{CO})_9]$ and $[\text{Fe}_3(\text{CO})_{12}]$ which were previously synthesized laboratory stock. Commercial $\text{Me}_3\text{NO}\cdot 2\text{H}_2\text{O}$ was rendered anhydrous by azeotropic distillation in toluene and stored under argon. The complex $[\text{Ni}(\text{S}_2\text{C}_2\text{Ph}_2)_2]$ was prepared by the literature method.⁷¹

Caution: *Although we have no evidence for the formation of highly toxic $[\text{Ni}(\text{CO})_4]$ during these reactions, this possibility should be borne in mind during work up.*⁸⁶

Synthesis of $[\text{Fe}_2(\mu\text{-S}_2\text{C}_2\text{Ph}_2)(\text{CO})_6]$ (**1**; $\text{R}^1 = \text{R}^2 = \text{Ph}$).

A solution of $[\text{Ni}(\text{S}_2\text{C}_2\text{Ph}_2)_2]$ (0.7713 g, 1.41 mmol) in toluene (50 cm^3) was treated with $[\text{Fe}(\text{CO})_5]$ (0.68 cm^3 , 5.03 mmol) and heated to 80°C for 23 h in a thermostatically-controlled oil bath. The initially green solution rapidly became dark purple and then more slowly changed to an orange-red colour. After cooling to r.t. and addition of silica (about 5 g), the solvent was removed *in vacuo*. The solid was then loaded onto a chromatography column. Elution with light petroleum - CH_2Cl_2 (9:1) produced an orange-red band of product **1** (0.6061 g, 1.16 mmol, 82% based on Ni). Elution with a 4:1 mixture of the same solvents gave an unidentified purple band, which turns green on removal of the solvent; and with a 3:2 mixture a small band of starting nickel complex was eluted. Continued elution with a 2:3 mixture of these solvents gave a brown band due to

[{Ni(S₂C₂Ph₂)₆}] **2** (0.3958 g, 0.219 mmol, 93% based on Ni). Two further minor bands could be eluted with a 7:3 mixture of the same solvents but remain unidentified.

Alternatively, a solution of [Ni(S₂C₂Ph₂)₂] (0.7096 g, 1.30 mmol) and [Fe(CO)₅] (0.68 cm³, 5.03 mmol) in THF (100 cm³) was treated with Me₃NO (0.7896 g, 10 mmol). The green solution immediately turned purple, accompanied by gas evolution. It was then heated at 75 °C for 23 h. Chromatographic work-up as above gave **1** (0.5968 g, 1.14 mmol, 88% based on Ni).

Data for **1**: IR (hexane): 2077m, 2042s, 2005vs, 1990w cm⁻¹. ¹H NMR: δ 7.20, 7.02 (m, Ph). ¹³C NMR: δ 207.8 (CO), 150.2 (CPh), 135.1 (C_{ipso}), 128.9, 128.5, 127.3 (Ph). Mass spectrum *m/z* 523 (M⁺H)⁺. These data are in agreement with those reported previously.¹²

Data for **2**: IR(ATR): 3054w, 2953w, 1594w, 1483w, 1441w, 1175w, 1074w, 1029w, 761m, 738s, 692vs cm⁻¹. ¹H NMR: δ 7.54-6.98 (m, Ph). ¹³C NMR: d 145.7, 144.6, 141.6, 141.5, 141.4, 140.0, 138.6, 138.5, 138.4, 138.4, 138.0, 137.6 (CPh + C_{ipso}), 130.2-125.3 (m, Ph). Anal. calc. for C₈₄H₆₀Ni₆S₁₂·2CH₂Cl₂: C, 52.27; H, 3.24; S, 19.45. Found: C, 52.43; H, 3.59; S, 18.84%. Mass spectrum (ES⁺): *m/z* 1804.

Synthesis of [Fe₂(μ-S₂C₂Ph₂)(CO)₆] (**1**; R¹ = R² = Ph) from [Fe₂(CO)₉] or [Fe₃(CO)₁₂].

A solution of [Ni(S₂C₂Ph₂)₂] (0.8917 g, 1.64 mmol) and [Fe₂(CO)₉] (1.1897 g, 3.27 mmol) in toluene (50 cm³) was heated to 80 °C for 24 h. The color of the solution changed rapidly to purple and ultimately orange-red as before. Separation of the products by column chromatography as above produced **1** (0.6179 g, 1.18 mmol, 72% based on Ni). In a similar way, a solution of [Ni(S₂C₂Ph₂)₂] (0.7462 g, 1.37 mmol) and [Fe₃(CO)₁₂] (0.9010 g, 1.78 mmol) in toluene (50 cm³) was heated at 80 °C for 24 h. In this case the solution did not pass through a purple stage, but slowly turned to dark orange-red. The product **1** was isolated as above (0.7017 g, 1.34 mmol, 98% based on Ni).

Synthesis of [Fe(CO)₂(PPh₃)(S₂C₂Ph₂)] **3** from [Fe(CO)₅].

A solution of [Ni(S₂C₂Ph₂)₂] (0.5086 g, 0.937 mmol) and [Fe(CO)₅] (0.15 cm³, 1.09 mmol) in THF (100 cm³) was treated with Me₃NO (0.135 g, 1.76 mmol). A rapid color change to dark purple occurred. The solution was stirred for 15 min, then triphenylphosphine (0.2800 g, 1.07 mmol) was added, causing a further change to green. The solution was stirred overnight to ensure

complete reaction. After addition of silica (5 g) the solvent was removed *in vacuo* and the residue loaded onto a column. Elution with light petroleum - CH₂Cl₂ (9:1) produced an orange-red band of **1** (30.1 mg, 0.06 mmol) and a purple band, which was followed by a green band of residual [Ni(S₂C₂Ph₂)₂] (41.7 mg, 8% recovery), eluted with a 17:3 mixture of the same solvents. The major dark blue band of **3** was then eluted with a 3:1 mixture of the same solvents; the compound was recolumned to remove the last traces of [Ni(S₂C₂Ph₂)₂], giving a final yield of 341.9 mg (0.51 mmol, 59% based on Ni). When the reaction was repeated with one equivalent of Me₃NO, a slightly lower yield of 54% was obtained.

After the elution of the major product, the green complex [Ni₃(μ-S₂C₂Ph₂)₃(PPh₃)₂] **6** could be eluted with a mixture of CH₂Cl₂/acetone (19:1). It proved difficult to obtain this complex in a pure state due to persistent contamination by Ph₃P=O and Ph₃P=S impurities, but washing with ethyl acetate followed by crystallisation gave a solid in which they were absent in the mass spectrum. The yield so obtained was 70 mg (16%). Solutions gradually turn brown and decompose on exposure to air.

Data for **3**: IR(CH₂Cl₂): 2006s, 1952s cm⁻¹. ¹H NMR: δ 7.73-7.07 (m, Ph). ¹³C NMR: δ 212.4 (d, J = 10Hz, CO), 168.9 (CPh), 142.4 (C_{ipso} of Ph), 133.3-127.1 (m, Ph). ³¹P NMR: δ 67.6. Anal. calc. for C₃₄H₂₅FeO₂S₂P: C, 66.23; H, 4.06; S, 10.39. Found: C, 65.70; H, 4.17; S, 10.29%. Mass spectrum: *m/z* 617 (M+H)⁺.

Data for **6**: ¹H NMR: δ 7.35-6.82 (m, 58 H, Ph), 6.51 (d, 2 H, Ph). ¹³C NMR: δ 171.5 (CPh), 150.2, 142.2, 141.2, 140.1 (CPh + C_{ipso}), 134.6 (Ph), 131.2 (C_{ipso}), 130.5-125.9 (m, Ph). ³¹P NMR: δ 43.3 (s, br). Mass spectrum (ES⁺): *m/z* 1426 (M⁺); HRMS: Found *m/z* 1426.0485; calc. for C₇₈H₆₀Ni₃P₂S₆ *m/z* 1426.0528.

Reaction of [Fe₂(μ-S₂C₂Ph₂)(CO)₆] (**1**; R¹ = R² = Ph) with PPh₃

A solution of [Fe₂(μ-S₂C₂Ph₂)(CO)₆] (0.5229 g, 1.00 mmol) and triphenylphosphine (0.573 g, 2.18 mmol) in dichloromethane (110 cm³) was treated with Me₃NO (0.158 g, 2.10 mmol) and allowed to stir at room temperature for 19 h. The solvent was removed *in vacuo* and the residue absorbed onto silica and loaded onto a column. Elution with light petroleum - CH₂Cl₂ (9:1) gave a red band of the monosubstituted complex [Fe₂(μ-S₂C₂Ph₂)(CO)₅(PPh₃)] **4** (514.0 mg, 0.67 mmol, 67%). Elution with a 4:1 mixture of the same solvents gave a blue band due to the mononuclear

complex $[\text{Fe}(\text{S}_2\text{C}_2\text{Ph}_2)(\text{CO})_2(\text{PPh}_3)]$ **3** (70.0 mg, 0.11 mmol, 11%). This was followed by a brown band of the disubstituted complex $[\text{Fe}_2(\mu\text{-S}_2\text{C}_2\text{Ph}_2)(\text{CO})_4(\text{PPh}_3)_2]$ **5** (173.0 mg, 0.175 mmol, 17.5%), eluted with a 3:1 mixture of the same solvents.

Data for **4**: IR(hexane): 2052vs, 1996vs, 1985m, 1947w cm^{-1} . ^1H NMR: δ 7.67 (t, $J = 9.0$ Hz, 6 H), 7.32 (m, 9 H), 7.10 (t, $J = 7.2$ Hz, 2 H), 7.02 (t, $J = 7.4$ Hz, 4 H), 6.63 (d, $J = 7.5$ Hz, 4 H). ^{13}C NMR: δ 214.1 (d, $J = 8$ Hz, 2CO), 209.7 (3CO), 149.7 (CPh), 136.2 (d, $J = 40$ Hz, C_{ipso} of PPh_3), 136.0 (C_{ipso}), 133.6-127.8 (m, Ph). ^{31}P NMR: δ 61.6. Anal. calc. for $\text{C}_{37}\text{H}_{25}\text{Fe}_2\text{O}_5\text{S}_2\text{P}$: C, 58.73; H, 3.31; S, 8.47. Found: C, 58.57; H, 3.34; S, 8.22%. Mass spectrum: m/z 757 ($\text{M}+\text{H}$) $^+$.

Data for **5**: IR(CH_2Cl_2): 2000vs, 1954m, 1938s cm^{-1} . ^1H NMR: δ 7.61 (t, $J = 8.7$ Hz, 12 H), 7.25 (m, 20 H), 6.94 (t, $J = 7.4$ Hz, 2H), 6.79 (t, $J = 7.6$ Hz, 4 H), 6.31 (d, $J = 7.5$ Hz, 4 H). ^{13}C NMR: δ 215.7 (t, $J = 4$ Hz, CO), 148.8 (CPh), 136.8 (d, $J = 38$ Hz, C_{ipso} of PPh_3), 136.4 (C_{ipso} of Ph), 133.5-127.0 (m, Ph). ^{31}P NMR: δ 58.4. Anal. calc. for $\text{C}_{54}\text{H}_{40}\text{Fe}_2\text{O}_4\text{S}_2\text{P}_2 \cdot 1.5\text{CH}_2\text{Cl}_2$: C, 59.60; H, 3.85; S, 5.73. Found: C, 59.64; H, 4.08; S, 5.72%. Mass spectrum: m/z 991 ($\text{M}+\text{H}$) $^+$.

Reaction of $[\text{Fe}(\text{CO})_2(\text{PPh}_3)(\text{S}_2\text{C}_2\text{Ph}_2)]$ (**3**) with $[\text{Fe}(\text{CO})_5]$ and Me_3NO .

A solution of $[\text{Fe}(\text{CO})_2(\text{PPh}_3)(\text{S}_2\text{C}_2\text{Ph}_2)]$ (99.8 mg, 0.162 mmol) in THF (10 cm^3) was treated with $[\text{Fe}(\text{CO})_5]$ (0.1 cm^3 , 0.76 mmol) and Me_3NO (61.3 mg, 0.82 mmol). A rapid colour change occurred to murky green-brown. After stirring for 18 h, the solution was brown. Separation of the mixture by column chromatography gave an orange band due to **1** (43.3 mg, 0.083 mmol, 51%), eluted with light petroleum - CH_2Cl_2 (19:1); a red band due to **4** (48.5 mg, 39%) eluted with a 17:3 mixture of the same solvents; and a small amount of remaining **3**, eluted with a 7:3 ratio of the same solvents.

Associated content

Supporting Information

^1H , ^{13}C and ^{31}P NMR spectra and selected mass spectra of compounds reported in this paper, with summary tables of crystal data for complexes **2**, **3**, and **6** (PDF).

Accession codes

CCDC 1878620 (**2**), 1878621 (**3**) and 1878622 (**6**) contain the supplementary crystallographic data for this paper. These data can be obtained free of charge via

www.ccdc.cam.ac.uk/data_request/cif or by emailing data_request@ccdc.cam.ac.uk, or by contacting The Cambridge Crystallographic Data Centre, 12 Union Road, Cambridge, CB2 1EZ, UK; fax: +44 1223 336033.

Author Information

Corresponding author

*E-mail for M.J.M.: M.Morris@sheffield.ac.uk

ORCID

Michael J. Morris: 0000-0001-8802-9147

Notes

The authors declare no competing financial interest.

Acknowledgements

We thank the University of Sheffield for support, Dr. Simon Parker for performing the electrochemical experiments, and Mr. Thomas Wieczorek for assistance with some experiments.

References

1. Lubitz, W.; Ogata, H.; Rüdiger, O.; Reijers, E. Hydrogenases. *Chem. Rev.* **2014**, *114*, 4081–4148.
2. Tard, C.; Pickett, C. J. Structural and Functional Analogues of the Active Sites of the [Fe]-, [NiFe]-, and [FeFe]-Hydrogenases. *Chem. Rev.* **2009**, *109*, 2245–2274.
3. Liu, X.; Ibrahim, S. K.; Tard, C.; Pickett, C. J. Iron-only hydrogenase: Synthetic, structural and reactivity studies of model compounds. *Coord. Chem. Rev.* **2005**, *249*, 1641–1652.
4. Heinekey, D. M. Hydrogenase enzymes: Recent structural studies and active site models. *J. Organomet. Chem.* **2009**, *694*, 2671–2680.
5. Rauchfuss, T. B. Research on Soluble Metal Sulfides: From Polysulfido Complexes to Functional Models for the Hydrogenases. *Inorg. Chem.* **2004**, *43*, 14–26.
6. Tschierlei, S.; Ott S.; Lomoth, R. Spectroscopically characterized intermediates of catalytic H₂ formation by [FeFe] hydrogenase models. *Energy Environ. Sci.* **2011**, *4*, 2340–2352.
7. Apfel, U.-P.; Pétilion, F. Y.; Schollhammer, P.; Talarmin J.; Weigand, W. [FeFe] Hydrogenase Models: an Overview. In *Bioinspired Catalysis*; Schollhammer, P; Weigand, W. Eds.; Wiley/VCH, Weinheim, 2014; Chapter 4, pp. 79–104.
8. Li, Y.; Rauchfuss, T. B. Synthesis of Diiron(I) Dithiolato Carbonyl Complexes. *Chem. Rev.* **2016**, *116*, 7043–7077.
9. Gao, W.; Ekström, J.; Liu, J.; Chen, C.; Eriksson, L.; Weng, L.; Åkermark B.; Sun, L. Binuclear Iron–Sulfur Complexes with Bidentate Phosphine Ligands as Active Site Models of Fe-Hydrogenase and Their Catalytic Proton Reduction. *Inorg. Chem.* **2007**, *46*, 1981–1991.
10. Li, P.; Wang, M.; He, C.; Li, G.; Liu, X.; Chen, C.; Åkermark B.; Sun, L. Influence of Tertiary Phosphanes on the Coordination Configurations and Electrochemical Properties of Iron Hydrogenase Model Complexes: Crystal Structures of $[(\mu\text{-S}_2\text{C}_3\text{H}_6)\text{Fe}_2(\text{CO})_{6-n}\text{L}_n]$ (L = PMe_2Ph , $n = 1, 2$; PPh_3 , $\text{P}(\text{OEt})_3$, $n = 1$). *Eur. J. Inorg. Chem.* **2005**, 2506–2513.
11. Ghosh, S.; Rahaman, A.; Holt, K. B.; Nordlander, E.; Richmond, M. G.; Kabir, S. E.; Hogarth, G. Hydrogenase biomimetics with redox-active ligands: Electrocatalytic proton

- reduction by $[\text{Fe}_2(\text{CO})_4(\kappa^2\text{-diamine})(\text{l-edt})]$ (diamine = 2, 2'-bipy, 1,10-phen). *Polyhedron* **2016**, *116*, 127–135.
12. He, J.; Deng, C.-L.; Li, Y.; Li, Y.-L.; Wu, Y.; Zou, L.-K.; Mu, C.; Luo, Q.; Xie, B.; Wei, J.; Hu, J.-W.; Zhao, P.-H.; Zheng, W. A New Route to the Synthesis of Phosphine-Substituted Diiron Aza- and Oxadithiolate Complexes. *Organometallics*, **2017**, *36*, 1322–1330.
 13. Abel-Futouh, H.; Almazahrez, L. R.; Kamal Harb, M.; Görls, H.; El-khateeb, M.; Weigand, W. [FeFe]-Hydrogenase H-Cluster Mimics with Various $-\text{S}(\text{CH}_2)_n\text{S}-$ Linker Lengths ($n = 2-8$): A Systematic Study. *Inorg. Chem.* **2017**, *56*, 10437–10451.
 14. Carroll, M. E.; Barton, B. E.; Rauchfuss, T. B.; Carroll, P. J. Synthetic Models for the Active Site of the [FeFe]-Hydrogenase: Catalytic Proton Reduction and the Structure of the Doubly Protonated Intermediate. *J. Am. Chem. Soc.* **2012**, *134*, 18843–18852.
 15. Wang, F.; Wang, W.-G.; Wang, X.-J.; Wang, H.-Y.; Tung, C. H.; Wu, L.-Z. A Highly Efficient Photocatalytic System for Hydrogen Production by a Robust Hydrogenase Mimic in an Aqueous Solution. *Angew. Chem. Int. Ed.* **2011**, *50*, 3193–3197.
 16. Liu, Y.-C.; Lee, C.-H.; Lee, G.-H.; Chiang, M. H. Influence of a Redox-Active Phosphane Ligand on the Oxidations of a Diiron Core Related to the Active Site of Fe-Only Hydrogenase. *Eur. J. Inorg. Chem.* **2011**, 1155–1162.
 17. Ott, S.; Kritikos, M.; Åkermark, B.; Sun, L. Synthesis and Structure of a Biomimetic Model of the Iron Hydrogenase Active Site Covalently Linked to a Ruthenium Photosensitizer. *Angew. Chem. Int. Ed.* **2003**, *42*, 3285–3288.
 18. Ekström, J.; Abrahamsson, M.; Olson, C.; Bergquist, J.; Kaynak, F. B.; Eriksson, L.; Sun, L.; Becker, H.-C.; Åkermark, B.; Hammarström, L.; Ott, S. Bio-inspired, side-on attachment of a ruthenium photosensitizer to an iron hydrogenase active site model. *Dalton* **2006**, 4599–4606.
 19. Ott, S.; Borgström, M.; Kritikos, M.; Lomoth, R.; Bergquist, J.; Åkermark, B.; Hammarström, L.; Sun, L. Model of the Iron Hydrogenase Active Site Covalently Linked to a Ruthenium Photosensitizer: Synthesis and Photophysical Properties. *Inorg. Chem.* **2004**, *43*, 4683–4692.
 20. Song, L.-C.; Tang, M.-Y.; Su, F.-H.; Hu, Q.-M. *Angew. Chem. Int. Ed.* **2006**, *45*, 1130–1133.

21. Samuel, A. P. S.; Co, D. T.; Stern, C. L.; Wasielewski, M. Ultrafast Photodriven Intramolecular Electron Transfer from a Zinc Porphyrin to a Readily Reduced Diiron Hydrogenase Model Complex. *J. Am. Chem. Soc.* **2010**, *132*, 8813–8815.
22. Song, L.-C.; Luo, F.-X.; Liu, B.-B.; Gu, Z.-C.; Tan, H. Novel Ruthenium Phthalocyanine-Containing Model Complex for the Active Site of [FeFe]-Hydrogenases: Synthesis, Structural Characterization, and Catalytic H₂ Evolution. *Organometallics* **2016**, *35*, 1399–1408.
23. Capon, J.-F.; Gloaguen, F.; Schollhammer, P.; Talarmin, J. Catalysis of the electrochemical H₂ evolution by di-iron sub-site models. *Coord. Chem. Rev.* **2005**, *249*, 1664–1676.
24. Gloaguen, F.; Rauchfuss, T. B. Small molecule mimics of hydrogenases: hydrides and redox. *Chem. Soc. Rev.* **2009**, *38*, 100–108.
25. Gloaguen, F. Electrochemistry of Simple Organometallic Models of Iron–Iron Hydrogenases in Organic Solvent and Water. *Inorg. Chem.* **2016**, *55*, 390–398.
26. Streich, D.; Karnahl, M.; Astuti, Y.; Cady, C. W.; Hammerström, L.; Lomoth, R.; Ott, S. Comparing the Reactivity of Benzenedithiolate- versus Alkyldithiolate- Bridged Fe₂(CO)₆ Complexes with Competing Ligands. *Eur. J. Inorg. Chem.* **2011**, 1106–1111.
27. Pandey, I. K.; Shaikh, S. M.; Deibel, N.; Sarkar, B.; Kaur-Ghumaan, S. Diiron Benzenedithiolate Complexes Relevant to the [FeFe] Hydrogenase Active Site. *Eur. J. Inorg. Chem.* **2015**, 2875–2882.
28. Chen, L.; Wang, M.; Gloaguen, F.; Zheng, D.; Zhang, P.; Sun, L. Tetranuclear Iron Complexes Bearing Benzenetetrathiolate Bridges as Four-Electron Transformation Templates and Their Electrocatalytic Properties for Proton Reduction. *Inorg. Chem.* **2013**, *52*, 1798–1806.
29. Streich, D.; Astuti, Y.; Orlandi, M.; Schwartz, L.; Lomoth, R.; Hammarström L.; Ott, S. High-Turnover Photochemical Hydrogen Production Catalyzed by a Model Complex of the [FeFe]-Hydrogenase Active Site. *Chem. Eur. J.* **2010**, *16*, 60–63.
30. Pullen, S.; Roy, S. Ott, S. [FeFe] Hydrogenase active site model chemistry in a UiO-66 metal–organic framework. *Chem. Commun.* **2017**, *53*, 5227–5230.
31. Lv, H.; Ruberu, T. P. A.; Fleischauer, V. E.; Brennessel, W. W.; Neidig, M. L.; Eisenberg, R. Catalytic Light-Driven Generation of Hydrogen from Water by Iron Dithiolene Complexes *J. Am. Chem. Soc.*, **2016**, *138*, 11654–11663.

32. Roy, S.; Mazinani, S. K. S.; Groy, T. L.; Gan, L.; Tarakeshwar, P.; Mujica, V.; Jones, A. K. Catalytic Hydrogen Evolution by Fe(II) Carbonyls Featuring a Dithiolate and a Chelating Phosphine. *Inorg. Chem.* **2014**, *53*, 8919–8929.
33. Kaur-Ghumaan, S.; Schartz, L.; Lomoth, R.; Stein, M.; Ott, S. Catalytic Hydrogen Evolution from Mononuclear Iron(II) Carbonyl Complexes as Minimal Functional Models of the [FeFe] Hydrogenase Active Site. *Angew. Chem. Int. Ed.* **2010**, *49*, 8033–8036.
34. Beyler, M.; Ezzaher, S.; Karnahl, S.; Santoni, M.-P.; Lomoth, R.; Ott, S. Pentacoordinate iron complexes as functional models of the distal iron in [FeFe] hydrogenases. *Chem. Commun.* **2011**, *47*, 11662–11664.
35. Gardner, J. M.; Beyler, M.; Karnahl, M.; Tschierlei, S.; Ott, S.; Hammarström, L. Light-Driven Electron Transfer between a Photosensitizer and a Proton-Reducing Catalyst Co-adsorbed to NiO. *J. Am. Chem. Soc.* **2012**, *134*, 19322–19325.
36. Orthaber, A.; Karnahl, M.; Tschierlei, S.; Streich, D.; Stein, M.; Ott, S. Coordination and conformational isomers in mononuclear iron complexes with pertinence to the [FeFe] hydrogenase active site. *Dalton Trans.* **2014**, *43*, 4537–4549.
37. Eady, S. C.; Breault, T.; Thompson, L.; Lehnert, N. Highly functionalizable penta-coordinate iron hydrogen production catalysts with low overpotentials. *Dalton Trans.* **2016**, *45*, 1138–1151.
38. Natarajan, M.; Faujdar, H.; Mobin, S. M.; Stein, M.; Kaur-Ghumaan, S. A mononuclear iron carbonyl complex $[\text{Fe}(\mu\text{-bdt})(\text{CO})_2(\text{PTA})_2]$ with bulky phosphine ligands: a model for the [FeFe] hydrogenase enzyme active site with an inverted redox potential. *Dalton Trans.* **2017**, *46*, 10050–10056.
39. Yap, C. P.; Hou, K.; Bengali, A. A.; Fan, W. Y. A Robust Pentacoordinated Iron(II) Proton Reduction Catalyst Stabilized by a Tripodal Phosphine. *Inorg. Chem.* **2017**, *56*, 10926–10931.
40. McNamara, W. R.; Han, Z.; Alperin, P. J.; Brennessel, W. W.; Holland, P. L.; Eisenberg, R. A Cobalt Dithiolene Complex for the Photocatalytic and Electrocatalytic Reduction of Protons. *J. Am. Chem. Soc.* **2011**, *133*, 15368–15371.

41. McNamara, W. R.; Han, Z.; Yin, C.-J.; Brennessel, W. W.; Holland, P. L.; Eisenberg, R. Cobalt-dithiolene complexes for the photocatalytic and electrocatalytic reduction of protons in aqueous solutions. *Proc. Nat. Acad. Sci.* **2012**, *109*, 15594–15599.
42. Eady, S. C.; Peczonczyk, S. L.; Maldonado, S.; Lehnert, N. Facile heterogenization of a cobalt catalyst via graphene adsorption: robust and versatile dihydrogen production system. *Chem. Commun.* **2014**, *50*, 8065–8068.
43. Eady, S. C.; MacInnes, M. M.; Lehnert, N. Immobilized Cobalt Bis(benzenedithiolate) Complexes: Exceptionally Active Heterogeneous Electrocatalysts for Dihydrogen Production from Mildly Acidic Aqueous Solutions. *Inorg. Chem.* **2017**, *56*, 11654–11667.
44. Gan, L.; Groy, T. L.; Tarakeshwar, P.; Mazinani, S. K. S.; Shearer, J.; Mujica, V.; Jones, A. K. A Nickel Phosphine Complex as a Fast and Efficient Hydrogen Production Catalyst. *J. Am. Chem. Soc.* **2015**, *137*, 1109–1115.
45. Eckenhoff, W. T.; Brennessel, W. W.; Eisenberg, R. Light-Driven Hydrogen Production from Aqueous Protons using Molybdenum Catalysts. *Inorg. Chem.* **2014**, *53*, 9860–9869.
46. Rauchfuss, T. B. Synthesis of Transition Metal Dithiolenes. In *Dithiolene Chemistry (Prog. Inorg. Chem. Volume 52)*; Stiefel, E.I., Ed.; Wiley: Hoboken, NJ 2004, Chapter 1, pp. 1–54.
47. King, R. B. Organosulfur Derivatives of the Metal Carbonyls. IV. The Reactions between Certain Organic Sulfur Compounds and Iron Carbonyls. *J. Am. Chem. Soc.* **1963**, *85*, 1584–1587.
48. Miller, J.; Balch, A. L. 1,2-Dithiolene Complexes of Ruthenium and Iron. *Inorg. Chem.* **1971**, *10*, 1410–1415.
49. Bird, C. W.; Hollins, E. M. The reaction of 1,4-dithiols with iron carbonyls. *J. Organomet. Chem.* **1965**, *4*, 245–246.
50. Siebenlist, R.; Fruhauf, H.-W.; Kooijman, H.; Veldman, N.; Spek, A. L.; Goubitz, K.; Franje, J. 1,3-Dipolar cycloaddition to the Fe–S=C fragment 20. Preparation and properties of carbonyliron complexes of di-thiooxamide. Reactivity of the mononuclear (di-thiooxamide)Fe(CO)₃ towards dimethyl acetylenedicarboxylate. *Inorg. Chim. Acta* **2002**, *327*, 66–89.
51. Seyferth, D.; Henderson, R. S. Photochemically induced insertion of acetylenes into μ -dithiobis(tricarbonyliron). *J. Organomet. Chem.* **1979**, *182*, C39–C42.

52. Charreteur, K.; Kdider, M.; Capon, J.-F.; Gloaguen, F.; Pétilion, F. Y.; Schollhammer P.; Talarmin, J. Effect of Electron-Withdrawing Dithiolate Bridge on the Electron-Transfer Steps in Diiron Molecules Related to $[2\text{Fe}]_{\text{H}}$ Subsite of the $[\text{FeFe}]$ -Hydrogenases. *Inorg. Chem.* **2010**, *49*, 2496–2501.
53. Seyferth D.; Womack, G. B. Construction of Bidentate Organosulfur Ligands via $(\mu\text{-RC}\equiv\text{CS})(\mu\text{-SLi})\text{Fe}_2(\text{CO})_6$ Intermediates. *Organometallics* **1986**, *5*, 2360–2370.
54. Schrauzer, G. N.; Mayweg, V. P.; Finck, H. W.; Heinrich, W. Coordination Compounds with Delocalized Ground States. Bisdithiodiketone Complexes of Iron and Cobalt. *J. Am. Chem. Soc.* **1966**, *88*, 4604–4609.
55. Adams, H.; Morris, M. J.; Morris S. A.; Motley, J. C. Dithiolene transfer from nickel to a dimolybdenum centre: the first dithiolene alkyne complex. *J. Organomet. Chem.* **2004**, *689*, 522–527.
56. Adams, H.; Gardner, H. C.; McRoy, R. A.; Morris, M. J.; Motley J. C.; Torker, S. Heterometallic Dithiolene Complexes Formed by Stepwise Displacement of Cyclopentadienyl Ligands from Nickelocene with $\text{CpMo}(\text{S}_2\text{C}_2\text{Ph}_2)_2$. *Inorg. Chem.* **2006**, *45*, 10967–10975.
57. Adams, H.; Coffey, A. M.; Morris M. J.; Morris, S. A. Efficient Transfer of Either One or Two Dithiolene Ligands from Nickel to Ruthenium: Synthesis and Crystal Structures of $[\text{Ru}(\text{SCR}=\text{CPhS})_2(\text{PPh}_3)]$ and $[\text{RuCl}_2(\text{SCR}=\text{CPhS})(\text{PPh}_3)_2]$ (R = Ph, H). *Inorg. Chem.* **2009**, *48*, 11945–11953.
58. Mousser, H.; Darchen A.; Mousser, A. Unexpected fragmentation of phenyldithiobenzoate, formation and X-ray structure of $[\mu, \eta^2(\text{S,S})\text{-1,2-(dithio)-1,2-(diphenylethylene)]\text{diiron hexacarbonyl}$ complex *J. Organomet. Chem.* **2010**, *695*, 786–791.
59. Weber H. P.; Bryan, R. F. Metal-Metal Bonding in Co-ordination Complexes. Part II. The Crystal Structure of $\mu\mu'$ (*cis*-Stilbene- α,β -dithiolato)-bis(tricarbonyliron). *J. Chem. Soc. (A)* **1967**, 182–191.
60. Jones, C. J.; McCleverty J. A.; Orchard, D. G. Bis(trifluoromethyl)dithiolene Tricarbonyl Iron and its Lewis Base Derivatives. *J. Chem. Soc., Dalton Trans.* **1972**, 1109–1114.

61. Berry, F. J.; Jones, C. J.; McCleverty, J. A.; Sharpe, J.; Bailey N. A.; Deadman, M. Structural and Mössbauer investigations of some iron complexes containing both carbonyl and sulphur ligands. *J. Organomet. Chem.* **1988**, 353, 209–213.
62. Touchard, D.; Fillaut, J.-L.; Khasnis, D. V.; Dixneuf, P. H.; Mealli, C.; Masi, D.; Toupet, L. Electron Transfer from Borohydride and Selective Reductions of Iron Cations. Synthesis of Tetrathiooxalate Iron Derivatives. *Organometallics* **1988**, 7, 67–75.
63. Hall, G. B.; Chen, J.; Mebi, C. A.; Okumura, N.; Swenson, M. T.; Ossowski, S. E.; Zakai, U. I.; Nichol, G. S.; Lichtenberger, D. L.; Evans, D. H.; Glass, R. S. Redox Chemistry of Noninnocent Quinones Annulated to 2Fe2S Cores. *Organometallics* **2013**, 32, 6605-6612.
64. The parameter τ is defined as $\beta - \alpha/60$, where α and β are the two largest bond angles and the apical ligand is defined as the one not involved in either of these. The value of τ therefore varies between 0 for a perfect square based pyramid and 1 for a perfect trigonal bipyramid. Addison, A. W.; Rao, T. N.; Reedijk, J.; van Rijn, J.; Verschoor, G. J. Synthesis, Structure, and Spectroscopic Properties of Copper(II) Compounds containing Nitrogen-Sulphur Donor Ligands; the Crystal and Molecular Structure of Aqua[1,7-bis(N-methylbenzimidazol-2'-yl)-2,6-dithiaheptane]copper(II) Perchlorate. *J. Chem. Soc., Dalton Trans.* **1984**, 1349-1356.
65. Bernal, I.; Clearfield, A.; Epstein, E. P.; Ricci, J. S., Jun. Isomeric Conformations in a Pentaco-ordinated Ruthenium Compound; Crystal and Molecular Structures of the Orange and Violet Isomers of $(\text{Ph}_3\text{P})_2[(\text{CF}_3)_2\text{C}_2\text{S}_2]\text{Ru}(\text{CO})$. *J. Chem. Soc., Chem. Commun.*, **1973**, 39-40.
66. Bernal, I.; Clearfield, A.; Ricci, J. S., Jun. Crystal structure of the orange isomer of $(\text{Ph}_3\text{P})_2[(\text{CF}_3)_2\text{C}_2\text{S}_2]\text{Ru}(\text{CO})$. *J. Cryst. Mol. Struct.* **1974**, 4, 43-54.
67. Clearfield, A.; Epstein, E. P.; Bernal, I. The crystal and molecular structure of the violet isomer of $(\text{Ph}_3\text{P})_2[(\text{CF}_3)_2\text{C}_2\text{S}_2]\text{Ru}(\text{CO})$. *J. Coord. Chem.* **1977**, 6, 227-240.
68. Porter, T. M.; Wang, J.; Li, Y.; Xiang, B.; Salsman, C.; Miller, J.S.; Xiong, W.; Kubiak, C.P. Direct observation of the intermediate in an ultrafast isomerization, *Chem. Sci.*, **2019**, 10, 113-117.
69. Makouf, N.B.; Mousser, H.B.; Darchen, A.; Mousser, A. Carbon monoxide substitutions by trimethyl phosphite in diiron dithiolate complex: Fe-Fe bond cleavage, selectivity of the

- substitutions, crystal structures and electrochemical studies. *J. Organomet. Chem.* 2018, 866, 35-42.
70. McCleverty, J. A.; Ratcliff, B. Transition-metal dithiolene complexes. XIV. Five coordinate phosphine and phosphite adducts of cobalt and iron bis(diaryl-1,2-dithiolenes). *J. Chem. Soc. (A)* **1970**, 1631–1637.
 71. Schrauzer, G. N.; Mayweg, V. P. Preparation, Reactions, and Structure of Bisdithio- α -diketone Complexes of Nickel, Palladium, and Platinum. *J. Am. Chem. Soc.* **1965**, 87, 1483–1489.
 72. Schrauzer G. N.; Rabinowitz, H. N. Charge Distribution and Nucleophilic Reactivity in Sulfur Ligand Chelates. Dialkyl Derivatives of Nickel (II), Palladium(II), and Platinum(II) Bis(*cis*)ethylenedithiolates. *J. Am. Chem. Soc.* **1968**, 90, 4297–4302.
 73. Ghosal, S.; Nirmal, M.; Medina J. C.; Kyler, K. S. Dithioannulation of alkynes. *Synth. Commun.* **1987**, 17, 1683–1694.
 74. Schrauzer, G. N.; Mayweg, V. P.; Heinrich, W. Coordination Compounds with Delocalized Ground States. α -Dithiodiketone-Substituted Group VI Metal Carbonyls and Related Compounds. *J. Am. Chem. Soc.* **1966**, 88, 5174–5179.
 75. Lim, B. S.; Donahue, J. P.; Holm, R. H. Synthesis and Structures of Bis(dithiolene)molybdenum Complexes Related to the Active Sites of the DMSO Reductase Enzyme Family. *Inorg. Chem.* **2000**, 39, 263–273.
 76. Goddard, C. A.; Holm, R. H. Synthesis and Reactivity Aspects of the Bis(dithiolene) Chalcogenide Series $[W^{IV}Q(S_2C_2R_2)_2]^{2-}$ (Q = O, S, Se). *Inorg. Chem.* **1999**, 38, 5389–5398.
 77. Nomura, M.; Okuyama, R.; Fujita-Takayama, C.; Kajitani, M. New Synthetic Methods for η^5 -Cyclopentadienyl Nickel(III) Dithiolene Complexes Derived from Nickelocene. *Organometallics* **2005**, 24, 5110–5115.
 78. Bosch, B. E.; Eisenhawer, M.; Kersting, B.; Kirschbaum, K.; Krebs, B.; Giolando, D. M. Synthesis, Properties, and Crystal Structures of Benzene-1,2-dithiolato Complexes of Thallium(I) and -(III). *Inorg. Chem.* **1996**, 35, 6599–6605.
 79. McLaughlan, C. C.; Ibers, J. A. Synthesis and Characterization of the Silver Maleonitrilediselenolates and Silver Maleonitriledithiolates $[K([2.2.2]-cryptand)]_4[Ag_4(Se_2C_2(CN)_2)_4]$, $[Na([2.2.2]-cryptand)]_4[Ag_4(S_2C_2(CN)_2)_4] \cdot 0.33MeCN$,

- [NBu₄]₄[Ag₄(S₂C₂(CN)₂)₄], [K([2.2.2]-cryptand)]₃[Ag(Se₂C₂(CN)₂)₂]₂·2MeCN, and [Na([2.2.2]-cryptand)]₃[Ag(S₂C₂(CN)₂)₂]. *Inorg. Chem.* **2001**, *40*, 1809–1815.
80. Beswick, C. L.; Terroba, R.; Greaney, M. A.; Stiefel, E. I. [PdS₂C₂(COOMe)₂]₆ⁿ (n = 0, -1, -2, -3, -4): Hexanuclear Homoleptic Palladium Dithiolene Complexes. *J. Am. Chem. Soc.* **2002**, *124*, 9664–9665.
81. Wrixon, J. D.; Hayward J. J.; Rawson, J. M. Phosphine Control of the Oxidative Addition Chemistry of Tetrathiocins to Palladium(0): Characterization of Mono-, Di-, and Hexanuclear Palladium(II) Dithiolate Complexes. *Inorg. Chem.* **2015**, *54*, 9384-9386.
82. Nakagawa, N.; Yamada, Y.; Murata, M.; Sugimoto, M.; Nishihara, H. Thermo-chromic Triangular [MCo₂] (M = Rh, Ir, Ru) Clusters Containing a Planar Metalladithiolene Ring in η³ Coordination. *Inorg. Chem.* **2006**, *45*, 14-16.
83. Nakagawa, N.; Murata, M.; Sugimoto, M.; Nishihara, H. Dithiolato-Bridged [MRu₂] (M = Rh, Ir, Ru) Triangular 50e⁻ Cluster Complexes Synthesized by Complete Metal Framework Reconstruction. *Eur. J. Inorg. Chem.* **2006**, 2129-2131.
84. Cha, M.; Sletten, J.; Critchlow, S.; Kovacs, J. A. Synthesis and structure of a thiolate-ligated Ni cluster which contains an unusual thiolate bridging mode and an exposed Ni site. *Inorg. Chim. Acta* **1997**, *263*, 153-159.
85. Cerrada, E.; Moreno, A.; Laguna, M. S, C- and S, S-coupling *via* dithiolate transfer reactions from tin to nickel complexes. *Dalton Trans.* **2009**, 6825-6835.
86. Solvents from reaction mixtures were collected in a liquid nitrogen cooled trap containing an excess of iodine and then allowed to warm to room temperature overnight. Both [Ni(CO)₄] and [Fe(CO)₅] are known to react with iodine.

Captions for Tables, Figures and Schemes

Figure 1. Structures of the dinuclear active sites of [FeFe]- and [NiFe]-hydrogenase enzymes.

Figure 2. Typical structures of di- and mononuclear models for the active site of the [FeFe]-hydrogenase.

Figure 3. Structure of diiron hexacarbonyl dithiolene complexes.

Figure 4. Molecular structure of [Fe(CO)₂(PPh₃)(S₂C₂Ph₂)] **3** in the crystal. Selected bond lengths (Å) and angles (°): Fe(1)–S(1) 2.1761(5), Fe(1)–S(2) 2.1942(5), Fe(1)–P(1) 2.2158(6), Fe(1)–C(33) 1.791(2), Fe(1)–C(34) 1.791(2), C(33)–O(1) 1.142(2), C(34)–O(2) 1.142(2), C(1)–C(2) 1.371(3); S(1)–Fe(1)–S(2) 88.18(2), S(1)–Fe(1)–P(1) 113.52(2), S(2)–Fe(1)–P(1) 94.05(2), C(33)–Fe(1)–S(1) 84.57(6), C(33)–Fe(1)–S(2) 167.01(6), C(33)–Fe(1)–P(1) 98.72(6), C(33)–Fe(1)–C(34) 91.27(9), C(34)–Fe(1)–S(1) 152.59(6), C(34)–Fe(1)–S(2) 90.23(6), C(34)–Fe(1)–P(1) 93.89(6).

Figure 5. Cyclic voltammogram of complex **3** in CH₂Cl₂ solution (room temperature, scan rate 100 mVs⁻¹).

Figure 6. Molecular structure of complex **2** in the crystal.

Figure 7. Schematic view of the framework of cluster **2** from the side (left) and top (right) of the molecule.

Figure 8. Cyclic voltammogram of complex **2** in CH₂Cl₂ solution (room temperature, scan rate 100 mVs⁻¹).

Figure 9. Structure of [Ni₃(μ-S₂C₂Ph₂)₃(PPh₃)₂] **6**.

Figure 10. Molecular structure of complex **6** in the crystal. Selected bond lengths (Å): Ni(1)–Ni(2) 2.4914(7), Ni(1)–Ni(3) 2.5125(8), Ni(2)–Ni(3) 2.5305(9), Ni(2)–S(1) 2.4767(12), Ni(3)–S(1) 2.1566(13), Ni(2)–S(2) 2.4500(14), Ni(3)–S(2) 2.1629(12), Ni(1)–S(3) 2.4959(12), Ni(3)–S(3) 2.1621(11), Ni(1)–S(4) 2.4147(13), Ni(3)–S(4) 2.1657(13), Ni(1)–S(5) 2.2840(13), Ni(2)–S(5) 2.2883(12), Ni(1)–S(6) 2.2975(13), Ni(2)–S(6) 2.2924(12), Ni(1)–P(2) 2.2720(11), Ni(2)–P(1) 2.2759(12), C(19)–C(20) 1.356(6), C(65)–C(66) 1.344(6), C(51)–C(52) 1.374(8).

Scheme 1. Synthesis of the iron dithiolene complexes by dithiolene transfer.

Scheme 2. Substitution reaction of complex **1** with PPh₃.